PROCEEDINGS OF SOCIETIES

THE CRYSTALLOGRAPHIC SOCIETY OF AMERICA

(JOINT MEETING WITH AMERICAN SOCIETY FOR X-RAY AND ELECTRON DIFFRACTION)

WILLIAM PARRISH, *Secretary-Treasurer,*
c/o Philips Laboratories, Inc., Irvington-on-Hudson, New York.

The third annual Spring meeting was held jointly with American Society of *X*-ray and Electron Diffraction at Yale University, New Haven, Conn., March 31–April 3. 1948. The meeting was attended by 205 people, 81 being members of C.S.A.

The officers for 1948 are:

President: Professor A. Pabst, University of California.

Vice-President: Professor J. D. H. Donnay, The Johns Hopkins University.

Secretary-Treasurer: Dr. William Parrish, Philips Laboratories, Inc.

Councilors: Professor N. W. Buerger, Postgraduate School, U. S. Naval Academy.
Professor I. Fankuchen, Polytechnic Institute of Brooklyn.

The Society now has 242 members, 25 residing outside U.S.A. Membership blanks may be obtained from the Secretary, c/o Philips Laboratories, Inc., Irvington-on-Hudson, N. Y. Abstracts of papers presented at the third annual meeting are given below.

A NEW MODIFICATION OF SODIUM

C. S. BARRETT, *University of Chicago.*

Employing techniques previously used on lithium,[1] samples of sodium (C.P. grade) were investigated at low temperatures in a Norelco spectrometer. After cold working at $-253°$ C. the diffraction pattern at $-195°$ C. showed a small diffraction peak in addition to the body-centered cubic pattern. Warming slightly caused the peak to disappear. If this peak is analogous to the similar one in cold-worked lithium it is the strongest line, (111), of the pattern of a face-centered cubic form of sodium. The face-centered cubic unit cell has a lattice constant equal to 5.339 Å at $-195°$ C.

That the proposed structure is reasonable is indicated by the atomic radius computed from this lattice constant, 1.880 angstroms, which may be compared with the value 1.874 Å computed from Pauling's radii for sodium in coordination 12, corrected to this temperature. The volume change is negligible, as in lithium: the calculated values for density are 1.012 for face-centered cubic sodium and 1.014 for body-centered cubic at $-195°$ C. Only about 1/10 of the sample has the new structure under the treatment employed.

[1] Barrett, C. S., *Phys. Rev.,* **72**, 245 (1947); Barrett, C. S., and Trautz, O. R., *A.I.M.E* Preprint, T.P. 2346, Metals Technology (**1948**).

THE NATURE OF THE ORDER OF LARGE SIZE EXHIBITED by COLLAGEN FIBRILS

RICHARD S. BEAR AND ORVIL E. A. BOLDUAN, *Massachusetts Institute of Technology.*

In order to explain the predominant small-angle diffraction effects obtained from dry tendon fibers, it is necessary to assume for the typical constituent fibril a model which has the following characteristics: while the fibril is approximately a smooth cylinder of finite width (diameter ca. 1000 Å) possessing predominantly longitudinal periodic structure, it is composed of smaller subfibrillar filaments (diameter ca. 100 Å) whose longitudinal structures are in approximate register, sufficient for diffraction in phase to low orders. Random small longitudinal displacements of the filaments progressively cause their diffractions to

fall out of phase, until at higher orders the diffraction effects are essentially those of individual filaments. Variations in effective radii of material diffracting to the higher orders indicate that the filaments themselves are not smooth but possess a periodically varying diameter.

STRUCTURAL CRYSTALLOGRAPHY OF LAZULITE, SCORZALITE AND VESZELYITE

L. G. BERRY, *Queen's University.*

The following new structural data for lazulite, scorzalite and veszelyite were obtained from single crystal photographs using the Weissenberg and Precession methods and copper radiation:

Lazulite and scorzalite: monoclinic—$P2_1/n$; the unit cell with $a = 7.12$, $b = 7.24$, $c = 7.10$ Å, $\beta = 118°55'$ (lazulite, Werfen, Salzburg). $a = 7.14$, $b = 7.27$, $c = 7.16$ Å, $\beta = 119°18'$ (lazulite, Graves Mt., Georgia). $a = 7.16$, $b = 7.25$, $c = 7.14$ Å, $\beta = 118°47'$ (lazulite, Churchill, Manitoba). $a = 7.15$, $b = 7.32$, $c = 7.14$ Å, $\beta = 119°00'$ (scorzalite, Minas Geraes, Brazil), contains 2 $[(Mg, Fe'')Al_2(PO_4)_2(OH)_2]$. Specific gravity, lazulite (Mg predominant) 3.06 to 3.12 (measured, various authors), 3.14 calculated for mineral with all Mg; scorzalite (Fe'' predominant) 3.33 (Pecora, 1947), 3.39 calculated for mineral with all Fe''. Cleavage ($\bar{1}01$) and (110) difficult. The morphological lattice (Dana 1892), is monoclinic $B2_1/a$ and pseudo-orthohexagonal.

Veszelyite: monoclinic—$P2_1/a$, the unit cell with $a = 9.84$, $b = 10.17$, $c = 7.48$ Å, $\beta = 103°25'$, $a:b:c = 0.9675:1:0.7355$, contains $4[(Cu, Zn)_3PO_4(OH)_3 \cdot 2H_2O]$. Specific gravity 3.34 (Zsivny), 3.531 (Schrauf), 3.42 calculated for Cu:Zn = 7:5. Cleavage (001). These data were obtained on a crystal fragment from Morawitza, Hungary. A chemical analysis of this material (Schrauf 1880) shows As substituting for P(P:As = 3:2). Later analyses of materials from other localities show no arsenic. X-ray powder photographs indicate structural identity of veszelyite from Morawitza and Vaskö, Hungary; and 'kipushite' from Kipushi, Belgian Congo.

ON THE CRYSTAL STRUCTURE OF AlPO₄

R. BRILL AND A. DEBRETTEVILLE, JR.,
Signal Corps Engineering Laboratories, Fort Monmouth, N. J.

AlPO₄ according to Huttenlocher[1] has a lattice similar to that of quartz. The lattice is hexagonal and has nearly the same a-axis (4.97_5 against 4.90_3 Å for quartz). The c-period is doubled (10.84 against $1/2 \times 10.78$ Å for quartz). The doubling of the c-spacings shows that Al and P layers alternate in planes parallel to the basal plane. In the possible space groups (see Huttenlocher) the different kinds of atoms have the following positions: Al: $3(a)$; P: $3(b)$; $O^I6(c)$; $O^{II}6(c)$. Under the assumption that the oxygen positions are the same as in quartz we get: $F_{003} = 3(A_1 - f_P)$ independent of the values of the different parameters. An absolute measurement of F_{003} should give some insight on the kind of chemical bond in AlPO₄, because $|f_{Al} - f_P|$ would be greater for neutral atoms (pure covalent bond-type) than for ions. Absolute intensity measurements were made of the basal plane reflections of AlPO₄. The crystals used were grown and prepared for our investigation by Mr. J. M. Stanley and Mrs. B. Korr of Squier Signal Laboratory. It can be shown that $1/3 \times F_{003}$ is about 8. This value is so high that it cannot be explained by a difference of the scattering power of even neutral Al and P-atoms. Therefore the positions of the two kinds of oxygen atoms cannot be equal. Preliminary measurements of the intensities of 006 and 009 show that the P-O distance is smaller than the Al-O distance. Therefore, a large amount of ionic bond may be present in AlPO₄.

[1] Huttenlocher, H. F., *Zeit. Krist.*, (A) **90**, 508–516 (1935).

CHEMICAL BOND OF MAGNESIUM OXIDE

R. Brill,

Signal Corps Engineering Laboratories, Fort Monmouth, N. J.

The oxides of the third row of the periodic system of elements show on the left side nearly pure ionic bond (Na_2O), and on the right side covalent bond (Cl_2O_7). In the middle of that row (SiO_2), we have nearly 50% ionic and 50% covalent bond.

Investigation of magnesium oxide was made using the Fourier synthesis method to see whether a certain amount of covalent bond may be found in magnesium oxide. Investigation shows that the electron background in the whole lattice is greater than in all investigated alkaline halides. Three dimensional Fourier synthesis showed that the electron density does not decrease below 0.15 electrons per A^3 at any point of the lattice. In sodium chloride the lowest electron density was 0.006 electrons A^3. The difference cannot be caused by a higher thermal movement in MgO. Furthermore, the intensity measurements showed that the atomic scattering factor of magnesium ion at low angles is smaller than the theoretical values. Also that for oxygen ion is slightly larger than the theoretical values. This means that the magnesium ions are little more expanded and the oxygen ions slightly more contracted. All these results show that there is a certain amount of covalent bond in magnesium oxide. The investigation was carried out together with Dr. Herman and Dr. Peters.

CRYSTALS BASED ON THE SILICA STRUCTURES

M. J. Buerger,

Massachusetts Institute of Technology.

Some 15 compounds are known to occur in crystals whose structures are derivatives[1] of quartz, tridymite, or cristobalite. These can be placed in two different categories: (1) half-breed derivatives, and (2) stuffed derivatives.

In the half-breed type, half the silicon positions are occupied by trivalent atoms, half by pentavalent atoms. If these atoms are ionic, then the electrostatic valence rule requires that the proxy atoms alternate in the structure in order that the sum of the valence bonds to the shared oxygen atoms be 2. Half-breed derivatives of the silica structures are known for BPO_4, $AlPO_4$, $FePO_4$, $BAsO_4$, and $AlAsO_4$. Quartz-, tridymite-, and cristobalite-like structures are known for various members of this group. All three types are known for $AlPO_4$.

In the stuffed type, one or more of the silicon atoms is replaced by an atom of lower valence, the valence balance being supplied by an alkali atom or atoms in interstitial spaces of the structure. Only in $LiAlSiO_4$ is the alkali atom small enough to be accommodated in the small interstitial spaces of a quartz-like structure. All other compounds have a tridymite-like or cristobalite-like structure because the larger voids of these structures are required to house the alkalis Na and K. Stuffed structures are known for $LiAlSiO_4$, $NaAlSiO_4$, $KAlSiO_4$, $BaAl_2O_4$; $Na_2Al_2O_4$, $K_2Al_2O_4$, $K_2Fe_2O_4$; Na_2CaSiO_4; also for minerals with more complex but related formulae: $KNa_3Al_4Si_4O_{16}$ (natural nepheline), $NaCaAl_3Si_{15}O_{36}$ (natural tridymite).

All these structures are derivative structures[1] and therefore have a lesser symmetry content per unit volume than the corresponding silica structures. This requires either multiple cells or lowered non-translational symmetry. This last feature is frequently accompanied by twinning which increases the apparent symmetry. Twinning of this sort occurs in $LiAlSiO_4$, $NaAlSiO_4$, and $KAlSiO_4$. The potassium salt has been supposed to be hexagonal, but diffraction data suggest that the apparently single crystals have orthorhombic or lower symmetry.

[1] Buerger, M. J., Derivative crystal structures: *J. Chem. Phys.*, **15**, 1–16 (1947).

New data are presented for LiAlSiO$_4$. Powder patterns and rotation photographs about both a and c indicate that this is a derivative of the quartz structure, but the failure of the 0001 extinction which occurs in quartz shows that its symmetry is less than hexagonal and that the apparently single crystals must be twins. The apparent cell edges derived from rotation and precession photographs are:

$$a = 10.55 = 2 \times 5.275 \text{ true Å.}$$
$$c = 11.22 = 2 \times 5.61 \text{ true Å.}$$

The apparent cell has both edges about double those of the quartz cell. The crystals of LiAlSiO$_4$, whose cell characteristics are reported above, were grown by the Washken Laboratories of Cambridge, Mass., under a development contract with the Squier Signal Laboratory, U. S. Army Signal Corps, Fort Monmouth, New Jersey.

PHASE DETERMINATION WITH THE AID OF IMPLICATION THEORY

M. J. BUERGER,
Massachusetts Institute of Technology.

Since the implication diagram provides the locations of atoms in crystals, there must be a close similarity between a Fourier representation of the implication diagram and the Fourier representation of the projection of electron density of the crystal on the same plane. The relation between the coefficients of the two series can be ascertained in several ways. A straightforward way which is not difficult in cases of low symmetry is to expand $FF^*(hkl)$ and then separate $F(h'k'l')$ from the rest of the expansion. For symmetries other than $\bar{1}$ it is then possible to eliminate most (if not all) of the unsymmetrical components. This is illustrated for symmetry 2 parallel to c, as follows: By a simple manipulation, the expansion of $FF^*(hkl)$ can be arranged in the following form:

$$F_{hkl}^2 = Q + F_{hkl}(P_0) + F_{hkl}(P_z) + Rf_{2h,2k,0} + \sum_j (R_j - R_i) F_{2h,2k,0}^1 \qquad (1)$$
$$\quad\;\; \text{(a)} \qquad \text{(b)} \qquad\;\; \text{(c)} \qquad\; \text{(d)} \qquad\quad\;\; \text{(e)}$$

where

$$Q = \sum_j N_j f_j, \quad N = \text{rank of equipoint}$$

and

$$R = \frac{f_{hkl}^2}{f_{2h,2k,0}} \, .$$

The expansion consists of five parts, which can be described in terms of the contribution of this term to the Patterson synthesis. (a) is a contribution to the origin peak, (b) represents the contribution on the Harker level to a non-Harker peak, and (c) represents a contribution on a non-Harker level to a general Patterson peak.

Term (c), which represents a very large part of the expansion, can be eliminated by the following manipulation: All terms are summed over l from $l = -L$ to $+L$, and each side of the equation is multiplied by $\cos 2\pi(kx+hy)$. The left side of (1) then represents the hk contribution to a Harker synthesis on level zero, and the parts of the right side of (1) represent the hk contributions to Fourier syntheses of quasi-electron density representations. In the complete syntheses, (c) vanishes because it represents a section on level zero, where there is no "density." The only way for this to occur is for each term, $\sum_l F(P_z)$ to vanish independently. This eliminates the term $\sum_l F_{hkl}(P_z) \cos 2\pi(hx+ky)$. All terms are now divided by $\cos 2\pi(hx+ky)$. There remains

$$\sum_l F_{hkl}^2 = \sum_l Q + \sum_l F_{hkl}(P_0) + \sum_l RF_{2h,2k,0} + \sum_l \sum_j (R_1 - R_j)F_{2h,2k,0}. \qquad (2)$$

$$\quad (a) \qquad\quad (b) \qquad\qquad\quad (d) \qquad\qquad\quad (e)$$

When non-Harker peaks can be recognized on the implication map, for example, by the non-appearance of satellites in certain symmetries, term (b) can be allowed for. Relation (2) then provides the relation of F's to F^2's for two-fold symmetry. The last term is a correction term which arises due to the fact that all atoms do not scatter with the same power. When all atoms have about the same scattering power, as in many organic compounds and in many silicates, this term vanishes. In other cases, it can be evaluated from special position information, or more generally, from the locations of certain atoms provided by the implication diagram. Where these do not apply, then this term can be evaluated for its maximum value, in which case it sets determinable limits on the part of (2) which cannot be directly computed. Since the absolute values of the F's are known, it should not be difficult in most cases to decide on phases of the F's with the aid of (2).

Equalities of a similar nature exist for each Harker level of each symmetry. It should be noted that the phases of only a fraction of the coefficients of the electron density series can be determined in this way. The fraction is $\frac{1}{4}$, $\frac{1}{3}$, $\frac{1}{2}$, or 1, corresponding, respectively to the implication ambiguity of 4, 3, 2, and 1. Therefore, if an electron density map is computed using the terms whose coefficients are determined in this manner, n possible positions appear for each atom in the crystal structure, where n is the ambiguity coefficient of the implication. The wrong positions can only be removed by supplying the electron density series with the missing terms.

VIBRATIONS OF CRYSTALS*

NICHOLAS CHAKO,
Alabama Polytechnic Institute.

In recent years extensive theoretical and experimental studies have been made of the vibrational properties of crystals, with particular reference to quartz, tourmaline and rochelle salt.[1] Recently, extensive theoretical investigations have been carried out on quartz plates and the calculated vibrations have been found in agreement with experiment.[2,3] However, because of the complexity of the problem, only the simplest types of crystals have been considered, and the treatment has been limited to certain cuts and to the simplest geometrical figures. Calculations of the vibration characteristics have been carried out for rectangular and circular plates, both of quartz[2,3,4,5], and rochelle salt.[5]

For circular plates one applies Love's theory for the calculation of extensional vibrations. It is found that the contribution of the piezoelectric terms in the calculation of characteristic frequencies are negligible for the case of quartz (less than a fraction of one per cent) whereas for rochelle salt they amount to a significant fraction of the purely elastic frequency. There exist pure shear frequencies when the direction of the electric field makes small angle ($<5°$) from the Z axis of the crystal, and these have about the same frequencies as the elastic frequencies. For larger angles there exist no pure shears, and the vibrations

[1] Cady, W. G., Piezoelectricity (1946); Heising, R. A., Quartz Crystals, (1946).

[2] Bechmann, H., *Zeit. Physik*, **117**, 180 (1940); **118**, 515 (1941); **120**, 107 (1942).

[3] Mason, Sykes, Bond, in Bell Telephone Technical Journal (See Heising, l.c.)

[4] Ekstein, H., *Phys. Rev.*, **66**, 105 (1944); **68**, 11 (1945); **70**, 76 (1946).

[5] Chako, N., *Phys. Rev.*, **71**, 470 (1947).

are no longer of a simple harmonic type. In case of rochelle salt, one finds that the vibrations are not a pure harmonic type, and only for large values of the characteristic number do they become of an harmonic character. The thickness vibration of the latter are found to be non-degenerate.

THE BEHAVIOR OF PUNCH FIGURES IN THALLIUM HALIDE CRYSTALS

J. W. DAVISSON AND B. HENVIS,
Naval Research Laboratory.

The penetration of a pointed instrument such as a scriber into a thallium halide crystal results in surface dislocations called punch figures and also in preferential volume displacements. It will be shown that both the surface and volume effects are due to slip in the [100] directions.

When a [100] direction lies close to the surface, slight penetration of the scriber will produce surface dislocations extending about an inch in the [100] directions. The surface dislocations diminish in length in proportion to the degree of dip of the [100] directions. This behavior results in an extreme sensitivity of the punch figure in the neighborhood of a [100] pole. Thus it is possible to locate the [100] poles and the [100] directions on hemispherical surfaces of these crystals with precision.

Slight penetration of a (100) section $\frac{1}{4}''$ thick by means of a lead pencil produces a small pip or protuberance on the opposite surface. Similarly penetration of a $\frac{1}{4}''$ (110) section results in two pips corresponding to the two 45° [100] directions. The pips formed in the (110) sections are diamond based pyramids with well defined steps. These structures are formed by gliding of (110) planes in the [100] directions.

Contrary to the general rule established for metals, slip in the body-centered thallium halide crystals does not take place in the direction of greatest linear atomic density, but along rows of similar ions.

PERMANENT POLARIZATION OF A SINGLE CRYSTAL OF BARIUM TITANATE

A. DEBRETTEVILLE, S. BENEDICT LEVIN, AND H. ESTELLE,
Signal Corps Engineering Laboratories.

A very small barium titanate crystal was silvered on two edges, mounted on a microscope slide, fitted with snug-fitting aluminum foil electrodes and a close iron-constantan thermocouple, and set in a micro-oven for continuous observation in polarized light. By a combination of heating and cooling in a strong DC field the crystal was detwinned and rendered optically homogeneous, having apparent biaxial negative character and acute bisectrix c coincident with the axis of dielectric polarization.

By connecting the crystal into an oscillograph circuit, the ferro-electric hysteresis loop of the crystal was observed at 15 volts 60 cycle AC, with and without an additional positive DC bias. By raising the crystal above 65° C, and cooling in a field of 2000 volts/cm. for 5 minutes and then removing the field, the crystal retained a charge which apparently is a volume polarization. This is exhibited as a distortion of the hysteresis loop. The polarity of the charge is the same as that of the formerly applied field.

The minimum temperature for which a charge will be retained, using the above fields and times is 65° C. A charge has been retained for over 80 hours, though diminished, by cooling from above the transition point with 2,500 volts/cm. initial field. Cherry[1] and Adler have obtained a somewhat similar effect for poly-crystalline barium titanate.

[1] Cherry, W. L., Jr., Adler, Robert, *Phys. Rev.,* **72,** 981–982 (1947).

ATACAMITE TWINNING RE-EXAMINED

J. D. H. Donnay,

The Johns Hopkins University.

Ford's twin law (*Am. J. Sci.*, **30**, 16, 1910) may be defined in several ways. Results of calculations made from the Zepharovitch-Klein fundamental angles (in Dana) confirm those of Friedel (*Bull. Soc. fr. Min.*, **35**, 45, 1912), who used Ungemach's axial ratios (*ibid.*, **34**, 148, 1911). The space group and unit-cell dimensions, predicted from morphology and checked by Weissenberg photographs, agree with previous x-ray results (Thoreau and Verhulst, *Ac. Roy. Belgique, Bull.*, **24**, 716, 1938). It is not necessary to use Ford's irrational definition. Using –[950]– as 3-fold twin axis, the obliquity is zero (within limits of accuracy), but the index is 61. Using –[544]– as 2-fold twin axis, the obliquity is 3°46' and the index is 81. Such values for the twin index are abnormally high. The case is not closed!

GROPING STAGES IN SOME ORGANIC CRYSTAL STRUCTURE DETERMINATIONS

J. D. H. Donnay and C. P. Fenimore,

The Johns Hopkins University.

If an organic compound has a molecular crystal structure and if its molecules are fairly rigid, then the groping stages consist in finding the approximate position and orientation of these molecules in the unit cell. Among the many ways of attacking the problem, departures from the generalized law of Bravais, optical data, a knowledge of which planes reflect most intensely, as well as purely metrical considerations, may locate the molecules so closely that the structure can then be completed by Fourier methods. Even in the absence of heavy atoms, Patterson and Patterson-Harker syntheses may be useful checks for proposed arrangements.

Examples. The structure of orthorhombic dibiphenylene ethylene has been solved by such methods. It is shown approximately to possess a layer structure (001) by its large negative birefringence and acute bisectrix perpendicular to (001). A rough measure of the crystal pleochroism suggests that if the molecule is planar, the molecular planes are inclined $40° \pm 5°$ to (001). The crystal violates the generalized law of Bravais inasmuch as the observed $\{hk0\}$ forms are $\{130\}$ dominant and $\{200\}$ narrow; while $\{020\}$ and $\{110\}$, which should precede these in importance, are absent. A pseudo thirding of the b-axis allows an arrangement of molecular centers which accounts for the morphological anomalies, is compatible with the optical data, and is in agreement with Patterson and Patterson-Harker syntheses. A consideration of the most intensely reflecting planes of high indices leads to the orientation of the molecules in the xy and yz planes, essentially solving the structure.

Use of metrical considerations is illustrated by triclinic dipentaerythritol. The eminent cleavage (010) and biaxial negative character with acute bisectrix perpendicular to (100) point to a layer structure, as is known pentaerythritol. The ether molecular model looks promising. Such molecules can be arranged in centrosymmetrical pairs, then in chains and layers by repetition of the process. The period of the chain (in A.U.) is $2.6 \times 4 = 10.4$ (observed $a_0 = 10.4$). The distance between chains is $2.6 \times 5 = 13.0$ (observed $c_0 \sin \beta = 13.4 \times 0.968 = 13.0$). The β angle would be arctan $5 = 78°41'$ (observed, $75\frac{1}{2}°$). Hydrogen bonds will strengthen the layers. Two layers will easily fit in $d(010) = 9.6$, accounting for the structural halving observed ($0k0$, k even only).

THE CALCULATION OF STRUCTURE FACTORS BY A PUNCHED CARD METHOD

JERRY DONOHUE AND VERNER SCHOMAKER,
California Institute of Technology.

A method for the rapid calculation on punched cards of the structure factors of x-ray crystal structure analysis has been developed. It makes use of the following IBM equipment: automatic reproducing punch (type 513), automatic multiplying punch (type 601), alphabetical accounting machine (type 405), and sorter (type 11).

The general expression for the structure factor:

$$F_{hkl} = \sum_j f_j e^{2\pi i(h_j + ky_j + lz_j)} \quad \text{(summation over the } j \text{ atoms in the unit cell)}$$

can by suitable manipulation be expressed in the following way:
$F_{hkl} = A_{hkl} + iB_{hkl}$ where A_{hkl} and B_{hkl} are of the form:

$$n \sum_j f_j \left\{ \begin{matrix} \cos \\ \text{or} \\ \sin \end{matrix} \; 2\pi hx_j \right\} \left\{ \begin{matrix} \cos \\ \text{or} \\ \sin \end{matrix} \; 2\pi ky_j \right\} \left\{ \begin{matrix} \cos \\ \text{or} \\ \sin \end{matrix} \; 2\pi lz_j \right\}.$$

These forms of course depend on the space group under consideration. The scheme of calculation is sufficiently flexible however to enable it to be applied to any space group.

The following packs of cards must be prepared on a hand punch before starting a calculation:

1. X-cos 2πX-sin 2πX. On this pack is punched values of X together with those of cos 2πX and sin 2πX and their signs. The argument X runs from 0.000 to 0.999 in intervals of 0.001. This pack is used in all calculations.

2. Form factors. This pack contains one card for every reflection being calculated, together with the values of the corresponding form factors of each kind of atom in the cell. This pack is used in all calculations for a given crystal.

3. Parameters. These packs contain one card for each atom for each h, k, and l observed together with the values of hx, ky, and lz for the atoms, where x, y, and z are the trial parameters. This pack is used only in a particular calculation.

The scheme of the calculation consists of punching a set of atom reflection cards—one card for each (non-equivalent) atom for each (hkl)—which contain the following pertinent information: crystal, trial, atom, h, k, l, f_{atom}, hx, ky, lz, cos $2\pi hx$, cos $2\pi ky$, cos $2\pi lz$, sin $2\pi hx$, sin $2\pi ky$, and sin $2\pi lz$. (The particular trigonometric functions punched depends on the expressions for A_{hkl} and B_{hkl}.) The foregoing is accomplished by the appropriate reproducing, sorting, and gang punching operations. The products are next obtained on the multiplying punch. Each card then contains the individual atomic contributions to A_{hkl} and B_{hkl}. The cards are then sorted and the values of A_{hkl} and B_{hkl} are printed with the tabulator. If desired, the atom reflection cards may also be listed on the tabulator so that the contributions of each atom to each reflection are quickly available for reference.

The above scheme has been used to calculate a set of about 600 (hkl) reflections for a crystal with space group $P2_12_12_1$, eight non-equivalent atoms in the general positions of the cell. The time required for the actual calculation is about 24 hours, approximately one-tenth of that required for doing the calculation with a hand operated calculator. The time-saving factor will in general vary with the number of reflections being calculated, the scheme being used, and the complexity of the crystal under investigation.

STATISTICAL FLUCTUATION OF INTENSITY IN DEBYE-SCHERRER LINES DUE TO RANDOM ORIENTATION OF CRYSTAL GRAINS

HANS EKSTEIN,
Armour Research Foundation.

In the Debye-Scherrer diagram of a stationary polycrystalline sample, the intensity distribution in the line is erratic because of statistical irregularities of the crystal grain orientation. If the only causes of line breadth are the natural spectral width of the primary radiation and the small size of the crystal grains (i.e., pure Fraunhofer diffraction), the statistics of the intensity distribution can be described analytically. The "experimental" line center can be defined as the center of gravity of the intensity curve. The mean deviation of the experimental line center and, thereby, the mean deviation of the measured lattice parameter are found to be proportional to $1/\sqrt{N}$ if N is the number of crystal grains. If the irradiated area rather than the number of grains is a given constant, the mean error of the measurement becomes a function of the grain diameter. For a typical case; i.e., 1 sq. mm. irradiated area of iron with $CoK\alpha$ (radiation and particles of 2×10^{-4} cm. in length, the relative error $\Delta d/d$ is found to be about 2×10^{-6}; i.e., about ten times smaller than that reported in precision measurements. This indicates that the crystal statistics is not the limiting factor for precision measurements.

In the limiting case of negligible statistical fluctuation, the intensity distribution is smooth and can be approximated by a resonance curve whose width

$$B = B_{\text{spectral}} + B_{\text{size}}$$

is the sum of two terms, one due only to the spectral width of the primary beam, the other term being the usual breadth due to the grain size alone.

ACHROMATIZATION OF DIFFRACTION LINES

HANS EKSTEIN AND STANLEY SIEGEL,
Armour Research Foundation.

Large diffracting angles are necessary for the precision determination of lattice parameters. The line will be wide at these angles because of the spectral impurity of the incident characteristic radiation, and this width will limit the accuracy with which the line center can be determined. The line can be narrowed as follows:

A diverging polychromatic beam is allowed to fall on the plane surface of a single crystal. The beam diffracted by this crystal will diverge and will contain a bundle of rays whose wave length range corresponds to the finite spectral width of the characteristic radiation. The polycrystalline sample is mounted normal to the ray of wave length λ_o. If a point source is used, the rays diffracted by the sample will converge to a focus.

The condition for achromatization can be shown to be:

$$V = F\left(1 + 2\,\frac{\tan\theta}{\tan\theta_m}\right)\left(-\frac{1}{\cos 2\theta}\right) + l\cdot\frac{\cos(\theta_m+\alpha)}{\cos(\theta_m-\alpha)}$$

where α is the angle between the normal to the diffracting plane of the monochromator and the plane surface which is being irradiated, θ_m is the Bragg angle for the ray of wave length λ_o which strikes the plane surface and diffracts from the plane whose spacing is d_m, θ is the Bragg angle for the ray of wave length λ_o diffracted by the polycrystalline sample, l is the distance between the x-ray source and the monochromator, F is the distance from the polycrystalline sample to the focus, and V is the distance from the monochromator to the polycrystalline sample.

If the x-ray source is of extent S, then the focus is of extent

$$S' = S \cos 2\theta \frac{\cos (\theta_m + \alpha)}{\cos (\theta_m - \alpha)}$$

which can be made very small by proper choice of α.

CRYSTAL STRUCTURES OF AMMONIUM AND POTASSIUM MOLYBDOTELLURATES

Howard T. Evans, Jr.,

Laboratory for Insulation Research, Massachusetts Institute of Technology.

In a previous report,[1] preliminary lattice constants were reported for ammonium and potassium molybdotellurates, and it was stated that crystals of these compounds are isostructural. The final unit cell and space group data show that they are not, but possess entirely different symmetries:

$(NH_4)_6TeMo_6O_{24} \cdot 7H_2O$, orthorhombic, mmm; $a_0 = 14.62$ Å, $b_0 = 14.91$, $c_0 = 14.26$; space group $Pnaa = C_{2h}^{10}$; $Z = 4$, density calc. 2.82, found 2.78.

$K_6TeMo_6O_{24} \cdot 7H_2O$, orthorhombic, mmm; $a_0 = 14.30$ Å, $b_0 = 14.95$, $c_0 = 14.26$; space group $Pcba = C_{2h}^{15}$; $Z = 4$, density calc. 3.15, found 3.05.

A set of Patterson maps prepared for the ammonium salt allowed only three possible models for the complex ion. Calculation of structure factors showed a reasonable agreement of observed and calculated intensities for only one of these models. The x, y and z parameters for the tellurium and molybdenum atoms in the ammonium and probably also the potassium crystals (with x and z interchanged) are: Te 0, 0, 0; Mo_I 0, 0.228, 0; Mo_{II} 0.113, 0.121, -0.168; Mo_{III} 0.113, -0.121, -0.168. The model accepted here is one originally proposed hypothetically by Anderson,[2] in which the molybdenum atoms lie in a hexagon about the tellurium atom at the center, and the oxygen atoms lie in two close-packed layers of twelve above and twelve below the plane of the hexagon.

[1] Evans H. T., Jr., *Am. Mineral.*, **32**, 687 (1947).

[2] Anderson, J. S., *Nature*, **140**, 850 (1937).

CRYSTALLOGRAPHY OF THE POLYMORPHIC FORMS OF BARIUM TITANATE[1]

Howard T. Evans, Jr., and Robinson D. Burbank,

Laboratory for Insulation Research, Massachusetts Institute of Technology.

Crystallographic measurements have been made on single crystals of barium titanate recently prepared in this laboratory. The habit, lattice dimensions and twinning of the cubic form, and the tetragonal modification formed by cooling the cubic crystals below the Curie point at 120° C. are described. The twinning of the tetragonal form on the (101) plane is demonstrated by means of Buerger precession photographs, and it is shown that all the observed domain structure in these crystals is generated by lamellar glide twinning on this plane.

New information on the hexagonal form is presented. The unit cell is hexagonal with $a_0 = 5.735$Å, $c_0 = 14.05$Å, space group $C6_3/mmc = D_{6h}^4$, and contains six units of $BaTiO_3$. It is shown that the structure contains close-packed BaO_3 layers as in the perovskite structure, but stacked in a different sequence. A six-layer repeat unit is found, with the sequence

ABCACB. In this structure, two-thirds of the TiO_6 octahedra are found to be joined in pairs by sharing a face, while the remaining octahedra are single, sharing corners with the double groups. The two titanium atoms in the double groups are strongly repelled and are separated by a distance of about 2.96Å. It is suggested that this feature may account for the difference in dielectric properties of the cubic and hexagonal forms. New polymorphs of barium titanate are predicted.

THE ELECTRONIC DIGITAL COMPUTER

H. H. GOLDSTINE,
Institute for Advanced Study.

A SIMPLE GNOMONIC TRANSPORTEUR FOR *X*-RAY LAUEGRAMS*

SAMUEL G. GORDON,
Academy of Natural Sciences of Philadelphia.

The indexing of Lauegrams requires transposition of the Laue spots (which are at tan 2θ) to tan θ (stereographic trace of plane-pole in F-Laue, and gnomonic plane-pole in B-Laue) or to $90°-\theta$ (gnomonic plane-pole of F-Laue). The geometry involved is simple: to the line through the Laue spot and the center of the Lauegram draw the unit circle (5 cm. radius for $D=5$ cm. in camera), tangent to the line at the center of the Lauegram. From the Laue spot draw a line through the center of the circle. Erect perpendiculars to this line, tangent to each side of the unit circle. It is easily proven that the intersections of these tangents with that of the tangent through the Laue spot and the center of Lauegram are the points required, θ and $90°-\theta$. A simple transporteur may be constructed by swivelling a carpenter's square to a straight-edge, such that the center of rotation is 5 cm. below the straight edge used to connect the Laue spot and center of Lauegram; and the vertical arm moves tangent to it at the required distance. Such a device was described by Clark and Gross in 1937 for plotting $90°-\theta$. However the vertical arm can be adjusted to any distance from the center of rotation, giving reductions to 4, 3, 2.5 or 2 cm. as desired. A shorter vertical arm, on the opposite side of the center is used for plotting θ. Since the device is simply an angle bisector, it can be used for converting gnomograms to stereograms.

* See *Am. Mineral.*, **33**, 634 (1948).

PROGRESS IN SILICATE STRUCTURES

ADDRESS OF THE RETIRING PRESIDENT OF THE CRYSTALLOGRAPHIC SOCIETY OF AMERICA

J. W. GRUNER,
University of Minnesota.

(*Printed in full in this issue*)

A TWO CURVED CRYSTALS MONOCHROMATOR FOR THE STUDY OF LOW ANGLE SCATTERING

A. GUINIER AND G. FOURNET,
Laboratorie d'Essais, Paris, France.
(*Read by I. Fankuchen*)

A two crystals spectrometer has already been used by various authors[1] for the study of *x*-ray scattering at *very* low angles, the sample being placed between the two crystals. We now use a double monochromator in a different way, in order to decrease the ratio of the parasitic scattering to the studied scattering.

With a single curved crystal monochromator the reflected beam is very intense, but the lamella which receive the total direct beam issued from the tube give rise to scattered radiation of appreciable intensity. Therefore it is necessary in low angle scattering experiments to reduce the aperture of the reflected beam by a system of slits and so partly to lose the advantages of the curved crystal.

When the reflected beam is again reflected by a second crystal the parasitic scattered radiation practically disappears, even in directions close to the direction of the main beam. According to a suggestion of Dr. J. W. M. DuMond, we tried to place two curved quartz crystals in such a way that the monochromatic beam reflected by the first crystal could be reflected by the second. With JOHANN monochromators,[2] in spite of the imperfect focalization every ray of the beam is reflected, but only when the crystals are in *antiparallel position* and have the *same curvature*. But with JOHANNSONN[3] monochromators, the focalization being theoretically perfect, both parallel and antiparallel positions are convenient. Theory and experiment show that the intensity of the final beam is greater in the second device than in the first.

We found experimentally that the energy of the beam which can be used for the study of low angle scattering is nearly the same with two curved crystals as with a single crystal. The loss due to the double reflection is balanced by the increase in aperture of the beam. In our apparatus we can now register reticular spacings below 250 Å, because the distance from sample to film is only 100 mm. We hope with dissymetric monochromators[4] to increase this distance and to register 600 Å spacings.

The double monochromator is associated with a demountable rotating anode tube allowing a load of 60 m.a., 35 KV upon a 1 mm.² focus. This powerful source allows the various adjustments of the second crystal to be made with a fluorescent screen, and has considerably reduced the exposure times. For example, a good small angle pattern of a 5% haemoglobin solution is obtained within 40 minutes.

[1] Fankuchen I., and Jellinek M., *Phys. Rev.*, **67**, 201 (1945).

DuMond J. W. M., *Phys. Rev.*, **72**, 83 (1947).

[2] *Zeit. Phys.*, **69**, 185, (1931).

[3] *Zeit. Phys.*, **82**, 507, (1933).

[4] Guinier, A., *Comptes Rendus*, **223**, 31, (1946).

IMPROVED GEIGER COUNTER SPECTROMETER

E. A. HAMACHER AND WILLIAM PARRISH,
Philips Laboratories, Inc.

A description of changes made in the Norelco spectrometer which markedly improves resolution by use of a new geometrical arrangement and intensity by use of mica window x-ray and Geiger tubes.

Resolution. The focal spot of the x-ray tube, 9×2.8 mm., with length perpendicular to the axis of specimen rotation[1] was 0.24 ×2.8 mm. in projection at $1\frac{1}{2}°$. By rotating the focal spot 90° in manufacturing the x-ray tube, the length of the focal spot is made parallel to the axis of rotation and is 9×0.07 mm. in projection. A set of Soller slits 1×25 mm. between source and specimen and 1×50 mm. between specimen and receiving slit limits the divergence to 4.6° and 2.3°, respectively. Bragg focussing is used in the plane parallel to the Soller slit foils. The angular aperture of the incident beam is 42′ and covers a 20 mm. wide sample at 10°2θ. The CuKα doublet is resolved on reflection from (10$\bar{1}$1) of a single quartz crystal plate and the width at half height of each line is about 3′. In a quartz powder sample, the doublet is noticeably separated in the reflection from (11$\bar{2}$0), $2θ=36.58°$ in recorded data.

Intensity. The Lindemann glass windows have been replaced by 0.0005" thick mica for x-ray and Geiger tubes. It has about the same absorption as 0.020" pure beryllium and is much less than Lindemann glass for 0.7 to 2.5 Å. By eliminating the intermediate graded glass seal, the inactive length of the counters has been reduced from 35 mm. to 2.5 mm. The optimum pressure for the Lindemann glass counters was 30 cm. (Hg) since higher pressures gave no higher counting rates due to absorption in the long inactive length, whereas 60 cm. (Hg) or more may be used with the mica window. The use of chlorine[2] rather than methylene bromide for a quenching agent gives a much larger sensitive area. The data shown below are based on calculations of the per cent of the x-ray beam transmitted through x-ray and Geiger tube windows and inactive length, which is absorbed in the 100 mm. active length of the counter. This is a measure of the efficiency and hence expected increase in counting rate of the system for the same geometry and power input of the x-ray tube.

|	$MoK\alpha$	$CuK\alpha$	$FeK\alpha$	$CrK\alpha$
Lind. 30 cm. Argon	7%	15	6	2
Mica 60 cm. Argon	14	55	48	34

[1] Friedman, H., *Electronics*, April **1945**.

[2] Liebson, S. H., *Phys. Rev.*, **72**, 18 (1947).

THE STRUCTURE OF TOURMALINE*

GABRIELLE E. HAMBURGER AND M. J. BUERGER,
Massachusetts Institute of Technology.

Earlier work[1] has shown that the space group of tourmaline is $R3m$. The dimensions of the cell, referred to hexagonal axes were given as $a = 15.93$, $c = 7.15$. This cell (whose volume is equal to that of 3 primitive rhombohedral cells) contained 3 formula weights of composition

$$\begin{vmatrix} Na \\ Ca \end{vmatrix} R_3 \begin{vmatrix} Al \\ Fe \end{vmatrix}_6 B_3 Si_6 O_{27}(O,OH,F)_4$$
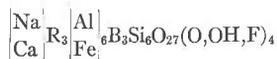
Intensity data were obtained for $(hkil)$ reflections for two comparatively simple tourmalines, namely for a black, Fe tourmaline from Andreasberg, and for a white, Mg tourmaline from de Kalb. In this study, the Weissenberg method was used with filtered cobalt and copper radiations, respectively, and the intensities were measured by the Dawton method.

From these data, implication diagrams $I3\ (xy0)$ were prepared for each crystal. In addition to satellites, both of these contained one very strong set of equivalent peaks. It seemed certain that this set was to be attributed to Si, Al, or both. In the preliminary form of this abstract, it was attributed to both. Subsequent intensity computations have shown that it is the location of Si only.

The difference implication, $\{I3\ (xy0)_{Fe} - I3\ (xy0)_{Mg}\}$ was also prepared. This displayed only one strong peak, which was obviously attributed to the Fe, Mg location. With the Si's and Mg's located in this manner, these atoms were surrounded by oxygen atoms consistent with their coordinations and with space requirements. This creates a segment of the structure of composition $NaMg_3Si_6O_{21}(OH)_4$. The Si_6O_{18} part of this segment is a ring of tetrahedra. The entire segment may be thought of as a fragment of the kaolin structure in which all octahedral positions are filled with Mg (instead of 2/3's of them being filled with Al). Na is located between these segments on the three-fold axis. The segments are joined together by Al octahedra which share some oxygens with the segment, but require 6 ad-

ditional oxygens in the general position. The Al octahedra spiral about the 3-fold screw axes sharing edges with each other. Boron is in planar triangular coordination.

Intensities of the (*hki*0) spectra computed for this structure are in excellent agreement with the observed intensities. The structure satisfies the Paulings rules, and the known wide range of tourmaline composition is explained by it.

The parameters for a tourmaline of composition $NaMg_3B_3Al_6Si_6O_{21}(OH)_4$ are as follows:

Atom	equipoint	x	y	z (approximate)
Na	3*a*	0	0	~7/9
Mg	9*b*	.133	.067	~1/6
B	9*b*	.117	.233	~ 0
Al	18*c*	.050	.367	~5/6
Si	18*c*	.192	.192	~5/9
$(OH)_1$	3*a*	0	0	~1/3
$(OH)_2$	9*b*	.233	.117	~ 0
O_1	9*b*	.058	.117	~ 0
O_2	9*b*	.142	.071	~2/3
O_3	9*b*	.102	.204	~2/3
O_4	18*c*	.200	.200	~1/3
O_5	18*c*	.279	.246	~2/3
O_6	18*c*	.058	.292	~ 0

* See *Am. Mineral.*, **33**, 532 (1948).

[1] Buerger M. J., and Parrish, William, The unit cell and space group of tourmaline: *Am. Mineral.*, **22**, 1139–1150 (1937).

HYPOTHETICAL DISORDER AND ITS USE IN CRYSTAL STRUCTURE DETERMINATIONS

DAVID HARKER,
General Electric Co.

Any crystal can be represented by the Fourier Series for its electron density:

$$\rho(x, y, z) = \frac{1}{V} \sum_h \sum_k \sum_l F_{hkl} e^{2\pi i (hx+ky+lz)},$$

where $F_{hkl} = F_{\bar{h}\bar{k}\bar{l}}$ (since $\rho(x, y, z)$ is real). The same structure shifted one-half unit translation along x is

$$\rho(x+\tfrac{1}{2}, y, z) = \frac{1}{V} \sum_h \sum_k \sum_l (-1)^h F_{hkl} e^{2\pi i (hx+ky+lz)}.$$

The average of these two structures is that of a crystal in which the two halves of the structure follow one another at random—a disordered structure. Its mean electron density is given by:

$$\rho_D(x, y, z) = \tfrac{1}{2}\big[\rho(x, y, z) + \rho(x+\tfrac{1}{2}, y, z)\big]$$

$$= \frac{1}{V} \sum_h \sum_k \sum_l \tfrac{1}{2}\big[1+(-1)^h\big] F_{hkl} e^{2\pi i (hx+ky+lz)}$$

$$= \frac{1}{V} \underset{\text{even}}{\sum_h} \sum_k \sum_l F_{hkl} e^{2\pi i (hx+ky+lz)}.$$

This structure is described by the Fourier coefficients with even h, i.e., it can be referred to a cell half as long in the x direction as the original one. The content of this half-sized cell consists of a superposition of the contents of the two halves of the true cell with the density scale divided by two.

It may happen in the early stages of a crystal structure determination that the disordered structure is more convenient to study than the ordered one. The final step in the determination then involves the "decollapse" of the structure into complete order. This process may not be unique, but the decision between the various possible ordered structures is made easily by means of the F_{hkl}'s not used for the disordered structure; e.g., by F_{hkl}'s with odd h in the example first described.

It is clear that disordering can be accomplished by superposition of thirds, fourths, etc., and that more than one axis can be used. The choice between various possible hypothetical disorderings is a matter of convenience. It happens frequently that the projection of a structure upon one of the crystallographically important planes can be described in terms of a smaller unit mesh than the true one; in such cases the use of a corresponding disordered structure is particularly convenient.

RELATIONS BETWEEN THE "PHASE INEQUALITIES", THE PATTERSON FUNCTION AND BUERGER IMPLICATIONS

DAVID HARKER,
General Electric Company.

To a crystal composed of real atoms can be related other periodic structures with the same unit cell. Thus, the crystal (C), the electron density of which is implied by the Fourier Coefficients F_{hkl}, can be related to the Patterson Function (P) with a density distribution implied by the Fourier Coefficients $|F_{hkl}|^2$. The P space contains "atoms" with coordinates $x_p - x_q$, $y_p - y_q$, $z_p - z_q$ where p and q are the ordinal numbers of the atoms in the C space. Another function related to the C-space is the Buerger Function (B) described by the Fourier Coefficients B_{hkl}. The B space contains some, but far from all, of the "atoms" belonging to the P-space; namely, those corresponding to atoms in C-space related by the operations of the space group of the real crystal.

An example may make this clearer. A crystal with the space group $P2$ has atoms at $x_j, y_j, z_j, \bar{x}_j, \bar{y}_j, \bar{z}_j$, where j runs from 1 to $N/2$ (N is the number of atoms in the unit cell of the real crystal). The corresponding Buerger Function has N "atoms" at 0, 0, 0 and at $2x_j, 0, 2z_j; 2\bar{x}_j, 0, 2\bar{z}_j$. The related Patterson Function has these "atoms" and many others with coordinates $x_p \pm x_q$, $y_p \pm y_q$, $z_p \pm z_q$ where p and q run over all the numbers from 1 to $N/2$ and the signs must be taken both plus or both minus. The unitary structure factors are (when written as sums over individual electrons):
for the crystal (C)

$$\widehat{F}_{hkl} = \frac{2}{Z} \sum_{j=1}^{z/2} e^{-2\pi i k y_j} \cos 2\pi (hx_j + lz_j),$$

for the Buerger Function (B)

$$\widehat{B}_{hkl} = \frac{1}{Z} \sum_{j=1}^{z/2} \left[1 + \cos 2\pi (2hx_j + 2lz_j) \right] = \widehat{B}_{h0l} = \tfrac{1}{2} + \tfrac{1}{2} \widehat{F}_{2h02l}$$

and for the Patterson Function (P)

$$\left| \widehat{F}_{hkl} \right|^2.$$

The Phase Inequality for a crystal of space-group P_2 is

$$\left| \widehat{F}_{hkl} \right|^2 \leq \tfrac{1}{2} + \tfrac{1}{2} \widehat{F}_{2h02l} \quad \text{or}$$

or

$$| \widehat{F}_{hkl} |^2 \leq \widehat{B}_{hkl}.$$

A section through P at $y=0$ will contain all "atoms" with $y \simeq 0$, but these include all the atoms in the same section through B, and it is these latter that are useful in determining the structure of C. The $\widehat{B}_{hkl's}$ in the P_2 case do not vary with k and for each h, l combination can be approximated by the largest $|\widehat{F}_{hkl}|^2$ for any k. From these can be calculated values of $B_{hkl} = \widehat{B}_{hkl}f^2$. The series evaluated from these coefficients should be more valuable in locating atoms in C than are the series using $|F_{hkl}|^2$'s. Similar relations hold for all space-groups, except $P1$ and $P\bar{1}$.

ABSOLUTE INTENSITY SCALE FOR CRYSTAL DIFFRACTION DATA

DAVID HARKER,
General Electric Company.

It is well known that the intensities I_{hkl} of the rays diffracted by a crystal can be calculated from its structure by the formula:

$$I_{hkl} = K\Phi(\lambda, \theta)|F_{hkl}|^2, \tag{1}$$

where h, k and l are the Miller indices of the sheaf of planes in the crystal from which the ray hkl can be said to have been "reflected"; λ is the wave length of the radiation used, θ is the glancing angle of "reflection," $\phi(\lambda, \theta)$ is a function dependent in form on the experimental arrangements, F_{hkl} is the "crystal structure factor" and K is a constant for a given specimen and radiation.

The "crystal structure factor," F_{hkl}, is related to the atomic arrangement in a crystal by the formula:

$$F_{hkl} = \sum_{j=1}^{N} f_j e^{-2\pi i (hx_j + ky_j + lz_j)}, \tag{2}$$

where N is the number of atoms in a unit cell of the crystal, $x_j, y_j,$ and z_j are the coordinates of the jth atom—expressed as fractions of the unit translations of the cell—and f_j is the scattering power of the jth atom. The values of f_j depend on $(\sin\theta)/\lambda$.

In the case of x-ray diffraction, it is possible to make the approximation $f_j = Z_j\widehat{f}$, where Z_j is the atomic number of the jth atom and $\widehat{f}$ is the same function of $(\sin\theta)/\lambda$ for all atoms. If $Z = \sum_{j=1}^{N} Z_j$ is the total number of electrons in the unit cell, we can define $\widehat{F}_{hkl} = F_{hkl}/Z\widehat{f}$ $\widehat{F}_{hkl}$ can be called the "unitary crystal structure factor" and can be calculated from the atomic arrangement of the crystal by the formula:

$$\widehat{F}_{hkl} = \sum_{j=1}^{N} n_j e^{-2\pi i (hx_j + ky_j + lz_j)} \tag{3}$$

where $n_j = Z_j/Z$ is the fraction of the electrons in the unit cell which belong to the jth atom. It is noteworthy that $\widehat{F}_{hkl}$ depends on the composition and structure of the crystal but not on the angle of diffraction or the wave length.

The intensities I_{hkl} and the known values of $\phi(\lambda, \theta)$ allow the calculation of the quantities $K|F_{hkl}|^2$ directly from the data, but, since the value of K is usually very inconvenient to measure experimentally, values of $|F_{hkl}|^2$ are obtained in most cases by calculation from the structure of the crystal. It will be shown in the following how the value of K may be obtained from the data with an accuracy depending on the validity of the relation $f_j = Z_j\widehat{f}$, even if the structure is not known.

The value of $|\widehat{F}_{hkl}|^2$ is obtained by multiplying (3) by its complex conjugate; the result is:

$$\left|\widehat{F}_{hkl}\right|^2 = \sum_{j=1}^{N} n_j^2 + \sum_{p=1}^{N} \sum_{\substack{q=1 \\ p \neq q}}^{N} n_p n_q e^{-2\pi i [h(x_p - x_q) + k(y_p - y_q) + l(z_p - z_q)]}. \qquad (4)$$

The mean value of $\left|\widehat{F}_{hkl}\right|^2$ over a large number of "reflections",[1] $\overline{\left|\widehat{F}_{hkl}\right|^2}$, is then given by

$$\overline{\left|\widehat{F}_{hkl}\right|^2} = \sum_{j=1}^{N} n_j^2 \qquad (5)$$

with a probable error of about $\pm 1/Q$, where Q is the number of "reflections" used in taking the average.[2]

Formula (5) is wrong only if $h(x_p - x_q)$, $k(y_p - y_q)$ and $l(z_p - z_q)$ are all integers or zero for all "reflections" used in averaging. If one is careful to average many non-cozonal "reflections," this cannot happen.

Since $\widehat{F}_{hkl} = F_{hkl}/Z\widehat{f}$, and writing $F'_{hkl} = KF_{hkl}$ for the "observed" structure factor, one obtains:

$$\overline{\left(\frac{\left|F'_{hkl}\right|^2}{Z^2\widehat{f}^2}\right)} = K \sum_{j=1}^{N} n_j^2$$

or

$$K = \overline{\left(\frac{\left|F'_{hkl}\right|^2}{Z^2\widehat{f}^2}\right)} \Bigg/ \sum_{j=1}^{N} n_j^2. \qquad (6)$$

The last relation can be rewritten

$$K = \overline{\left[\frac{\left|F'_{hkl}\right|^2}{\sum_{j=1}^{N} f_j^2}\right]}. \qquad (6')$$

The factor K, which converts the observed relative values of the squares of the "crystal structure factor," $\left|F_{hkl}\right|^2$, to the absolute scale can be evaluated from either (6) or (6').

The Temperature Factor: In the foregoing, it has been assumed that no thermal motion exists in the crystal under consideration, but this is never the case. The effect of this thermal motion on the intensities of diffraction can be allowed for by making K a function of $(\sin \theta)/\lambda$ according to the formula:

$$K = K_0 e^{-2B[(Sin\theta)/\lambda]}.[2]$$

In this case, it is no longer possible to use formulas (6) or (6') to obtain K, unless the "reflections" used in averaging all lie in a narrow range of $(\sin \theta)/\lambda$, and this value of K is useful only in that range. However, the variation of K with $(\sin \theta)/\lambda$ is such that a plot of lnK against $[(\sin \theta)/\lambda]^2$ is a straight line, with a slope of $(-2B)$ and an intercept on the axis of ordinates at lnK_0. Thus, if the values of K are computed from equations (6) or (6') in various ranges of $(\sin \theta)/\lambda$ and the results plotted as just suggested, not only can the intensities be referred to an absolute scale, but the temperature effect on intensity can be evaluated.

[1] A bar over a quantity is used to indicate the average value of that quantity.

[2] This follows from the expression

$$\frac{1}{2P+1} \sum_{n=-P}^{P} e^{-2\pi i \, nx} = \frac{1}{2P+1}\left(\frac{\sin \pi(2P+1)x}{\sin \pi x}\right).$$

GROWING CRYSTALS FROM SOLUTION

A. N. Holden,
Bell Telephone Laboratories.

Large clear single crystals of many ionic salts can be grown from water solution in a reciprocating rotary crystallizer. Seed crystals are moved at about fifteen inches per second through slowly cooled supersaturated solutions in cylindrical jars, heated at the bottom to dissolve spurious seed crystals. Practicable rates of clear growth reach a maximum of 200 molecular layers per second in favorable cases. These rates are controlled by the specific crystallization rate on the growing surfaces at the prevailing supersaturation and temperature, rather than by diffusion to them through the adjacent unstirred solution film, as can be shown (1) by comparison of growth rates with dissolution rates, and (2) by agreement in order of magnitude of observed rates and rates calculated from a rough kinetic theory. There is no satisfactory refined theory of crystallization in two-component systems, nor any adequate body of experimental data to verify one.

INDEX OF REFRACTION STUDIES OF ISOMETRIC OPAQUE MINERALS

Arthur L. Howland and M. Darwin Quigley,
Northwestern University.

The determination of the index of refraction of opaque substances by the application of Brewster's law was studied by Quirke and McCabe as a means for establishing a measure of the rank of coal. The same method has been applied by the authors to metallic oxides and sulfides such as magnetite, sphalerite, galena, and pyrite to determine its usefulness for the identification of opaque and high index minerals. The procedure followed was to determine the polarization angle by means of an analyzing prism and photometer when a beam of unpolarized light was directed against cleaved or polished surfaces of a mineral. Satisfactory checks were obtained with the known indices of glass, diamond, and sphalerite, but it was found that the nature of the surface is of great importance and that films of moisture or grease, and the destruction of the surface layers by polishing have a marked effect in lowering the values obtained. Index measurements were also obtained from the opaque minerals magnetite (2.42), galena (4.71), and pyrite (6.22), in contrast to metallic conductors such as silver and copper, for which the polarization angle cannot be determined by the experimental procedure employed. These minerals, which can be assumed to be representative of metallic oxides and sulfides, behave like dielectrics in permitting the maintenance of a coherent light beam for an appreciable depth beneath the surface.

THE PIEZOELECTRIC EFFECTS IN SOME UNIPOLAR CRYSTALS

Hans Jaffe,
*The Brush Development Company.**

The piezoelectric d_{nm} constants of several crystals having a unique polar axis are given. It is seen that the constants connecting an electric field *in* the polar axis to compressional strains are in the average somewhat smaller than the constants connecting fields *perpendicular* to the polar axis with various shear strains. The hydrostatic *piezoelectric* constant, however, which is the algebraic sum of 3 compressional constants, is generally quite small. Lithium sulfate monohydrate is a notable exception; its constant d_{22} relating field in polar direction to compressional strain in the same direction, is much higher than its other constants and gives rise to an outstanding hydrostatic effect.

A NEW PROCEDURE FOR CALCULATING RADIAL DISTRIBUTION CURVES FROM ELECTRON DIFFRACTION DATA

J. KARLE AND I. L. KARLE,
Naval Research Laboratory.

Radial distribution calculations have been rather inaccurate owing to the fact that experimental difficulties limit the amount of intensity data available for the integral ordinarily computed. The purpose of this paper is to indicate that the amount of intensity data usually obtained in scattering experiments is sufficient to accurately determine the structure of the scatterer by means of an inversion procedure and also to show how the calculation must be modified in order to accomplish this.

The integral required to determine the distribution of scattering matter $rf(r)$, is

$$f(r) = \sqrt{\frac{2}{\pi}} \int_0^\infty SI(S) \sin SrdS \tag{1}$$

where S is a function of the wavelength of the incident radiation and the angle of scattering and I is the experimentally determined intensity as a function of S. In practice the upper limit of integral (1) is S max determined by the maximum angle at which the intensity may be evaluated. The upper limit is ordinarily too small to give accurate results from (1). In order to overcome this difficulty for electron diffraction calculations, Degard,[1] Schomaker[2] and Finbak[3] have independently introduced a factor e^{-aS^2} into the integrand of (1) giving,

$$f_a(r) = \sqrt{\frac{2}{\pi}} \int_0^{S_{\max}} SI(S)e^{-aS^2} \sin SrdS. \tag{2}$$

The value of a can be chosen so that the integrand of (2) converges rapidly. The merit of this calculation is that the equilibrium distances between atoms are accurately determined and spurious peaks are eliminated. This is analogous to the use of an "artificial" temperature damping in the Fourier synthesis of crystal structure. The function $f(r)$ may be obtained from $f_a(r)$ by making use of the following relation,[4]

$$f_a(r) = \frac{1}{\sqrt{2\pi}} \int_{-\infty}^\infty f(\rho)m(r-\rho)d\rho \tag{3}$$

where the m function is the Fourier transform of e^{-aS^2}.

In order to study the internal motion of molecules it is necessary to evaluate $f(r)$ rather than $f_a(r)$. In our method $f_a(r)$ is first calculated from (2) and then $(f(r)$ is obtained from it using (3). In molecular scattering $f_a(r)$ often results in a series of well defined bell-shaped peaks. The introduction of an analytical $f(\rho)$ in the form of $e^{-h(r_0-\rho)^2}$ leads to an evaluation of integral (3), giving $f_a(r) = e^{-h(r_0-r)^2/4ah+1}/(4ah+1)^{1/2}$ which allows an immediate determination of $f(r)$ from $f_a(r)$.

The tests performed so far with this method indicate that with good intensity data, not only equilibrium distances but also the character of internal oscillations may be studied. Professor Verner Schomaker has very kindly made available to us a set of punched cards developed at the California Institute of Technology for performing the required numerical integrations.[5]

[1] Degard C., *Bull. Soc. Roy Sci. Liége,* **115**, (1938).

[2] Schomaker, V., presented to the *American Chemical Society,* Baltimore, April 1939.

[3] Finbak, Chr., *Tids. Kjemi, Bergvesen, Metallurgi,* **2**, 53 (1942).

[4] Titchmarsh, E. C., Introduction to the Theory of the Fourier Integral, Oxford, the Clarendon Press, page 51 (1937).

[5] Shaffer, P. A. Jr., Schomaker, V., and Pauling, L., *Jour. Chem. Phys.,* **14**, 659 (1946).

THE CRYSTAL STRUCTURE OF DECABORANE

J. S. Kasper, C. M. Lucht, and D. Harker,
General Electric Company.

The crystal structure of decaborane, $B_{10}H_{14}$, has been determined from single-crystal oscillation photographs, using $CoK\alpha$ x-radiation.

Crystals prepared by sublimation at room temperature, or above, show a high degree of polysynthetic twinning, giving rise to diffuseness of reflections for which h and k are odd. In the untwinned condition, the crystal is monoclinic,[1] but pseudo-orthorhombic, and it is convenient to choose the two-fold axis in the c direction. The space group is then $C_{2h}{}^4-C11$ $2/a$. With $a_0=14.37$ Å, $b_0=20.98$ Å, $c_0=5.69$ Å, $\beta=90.0°$, the cell contains eight molecules of $B_{10}H_{14}$, and the calculated density is 0.96.

The individual crystals, which make up the actual, highly twinned, crystalline edifice, are so short in the b-direction (a few unit translations, at most) that it is convenient to consider the system as a partially ordered crystal, the disordered state of which is described by a unit cell one-fourth the size of the one mentioned above. The dimensions of this small cell are: $a_0=7.18$ Å, $b_0=10.49$ Å, $c_0=5.69$ Å; and it contains $2B_{10}H_{14}$ or $(1/2$ B$)_{20}$ $(1/2$ H$)_{28}$. The "disordered" structure based on this cell explains *all* the sharp spots observed—its space-group is $D_{2h}{}^{12}-P_{nnm}$.

The boron parameters have been established by means of Fourier methods, including a three-dimensional synthesis of the complete unit cell. They have not varied more than $\pm.001$ in the last two refinements. Hydrogen atoms contribute significantly to many reflections, and it appears that all of them are resolved in Fourier sections. However, a total of 18 peaks, each possible for a hydrogen, has been obtained in the electron density functions for the molecule and the 14 hydrogen positions have not been assigned unequivocally at the present time. Consequently, only the boron parameters will be given. They are as follows (for the large unit cell of the ordered structure):

$$8B \text{ at } 000; \tfrac{1}{2}\tfrac{1}{2}0 +$$
$$xyz \qquad \tfrac{1}{2}+x, y, \bar{z}$$
$$\bar{x}\bar{y}\bar{z} \qquad \tfrac{1}{2}-x, \bar{y}, z$$

	x	y	z		x	y	z
B_I	.033	.328	0	B_I'	.217	.078	.500
B_{II}	.109	.276	.142	B_{II}'	.141	.026	.642
B_{III}	.109	.276	$-.142$	B_{III}'	.141	.026	.358
B_{IV}	.097	.202	0	B_{IV}'	.153	$-.048$	.500
B_V	.019	.210	.228	B_V'	.231	$-.040$	.728

The molecules are required by the space group to have only a two-fold axis, but appear to have two mirror-planes as well; thus, they exhibit the symmetry $C_{2v}-mm2$. From the coordinates listed above, the molecule of $B_{10}H_{14}$ has a novel, open-clam-shell type of structure which has not been postulated heretofore. Each boron atom is bound to five or six other atoms, but the bonds are not all equivalent. Tentatively, it appears that ten of the hydrogen atoms are each bound to a single boron atom; the four remaining ones may have a higher coordination number.

---

[1] Möller (*Zeit. Krist.*, **76**, 500–516, 1931) concluded incorrectly that the crystal class was orthorhombic. The correct space group, $C11$ $2/a$, is a sub-group of the one C_{mma}, given by Möller.

AN *X*-RAY CRYSTALLOGRAPHIC STUDY OF THE HYDRAZIDES OF SOME n-ALIPHATIC ACIDS

E. C. LINGAFELTER AND L. H. JENSEN,
University of Washington.

The hydrazides ($RCONHNH_2$) of hexanoic, heptanoic, and octanoic acids have been investigated by oscillation and equi-inclination Weissenberg photographs. The substances have the same structure, as predicted by Kyame, Fisher, and Bickford[1] from their melting point study. They are monoclinic (*Aa* or *A2/a*) with 8 molecules in the unit cell. The variation of d_{001} with chain length indicates that the axis of the chains must be nearly normal to (001), while a consideration of the intensities of (00*l*) reflections indicates that the chains are probably not exactly normal to (001). The average cross section of the chains appears to be slightly less than that of the *n*-paraffin hydrocarbons. The relation of the structure to those of other paraffin-chain compounds is discussed.

[1] Kayme, Fisher, and Bickford, *Jour. Am. Oil Chemists Soc.*, **24**, 332 (1947).

AN APPARATUS FOR OBTAINING A POWDER DIFFRACTION PATTERN FROM A SINGLE CRYSTAL

F. W. MATTHEWS AND A. O. McINTOSH,
Canadian Industries, Ltd.

A device which gives two complete simultaneous rotations to a single crystal is used to obtain diffraction patterns which simulate powder diffraction patterns. The relative intensity of the lines obtained is in reasonable agreement with those of the true powder pattern. The method may therefore be used for the identification of single crystals from published powder data. The method is useful in checking the identity of a crystal before proceeding with single crystal measurement. In metallurgical studies on coarse grained material powder measurements may be made in either the forward or back reflection region.

FERROELECTRIC ACTIVITIES OF BARIUM TITANATE

B. T. MATTHIAS,
*Massachusetts Institute of Technology.**

Dielectric and optical investigations of single crystals confirm the ferroelectric behavior of barium titanate. Several modifications have been obtained, of which only the pseudocubic shows ferroelectric anomalies, although all have unusually high dielectric constants.

The pseudocubic crystals exhibit a domain structure. In each domain the polarization vector lies along one of the cube edges, and thus in first approximation each domain has tetragonal symmetry, the optic axis being the direction of polarization. The optical observations are complicated by the fact that compatibility of strain due to differently directed polarization, distorts each domain from ideal tetragonality.

Dielectric measurements confirm the optical observations, and in particular show that sufficiently large electric fields can orient the polar axis of all the domains into the field direction. The polarizability for small field strength is about three times higher perpendicular to the polar axis than parallel to it. The ideal single domain crystal is tetragonal below the Curie Point without the necessity of applying a field. Under special growing conditions, however, crystals can be obtained which correspond rather completely to a perfect uniaxial crystal.

As the anisotropy of the crystal can be changed, with respect to fixed axes in the sample, so greatly by an applied electric field, the peculiar piezoelectric resonance behavior of barium titanate ceramics can be understood.

* Now at Bell Telephone Laboratories.

COLLECTION AND PUBLICATION OF CRYSTALLOGRAPHIC DATA

W. C. McCRONE,
Armour Research Foundation.

MORPHOLOGICAL AND OPTICAL CHARACTERIZATION OF ORGANIC CRYSTALS

W. C. McCRONE,
Armour Research Foundation.

HIGH INTENSITY GEIGER-COUNTER SPECTROMETER WITH EXTENDED ANGULAR RANGE

WILLIAM PARRISH AND E. A. HAMACHER,
Philips Laboratories, Inc.

Description of the redesigned Norelco Diffraction Unit arranged for simultaneous use with various types of cameras and a new Geiger counter spectrometer-type goniometer designed to scan in the vertical plane. The x-ray tube is water-cooled and has four mica windows. It is run at about 7 times greater power input (for copper target) than the air-cooled spectrometer x-ray tube. This higher intensity allows a faster scanning speed, or greater precision for the same scanning speed due to faster averaging of the counting statistics. Full-wave rectification gives a greater linear range in the intensity measurements with the Geiger tube and allows the use of a Sorensen electronic voltage regulator on the input line.

The use of the vertically-mounted x-ray tube and goniometer makes it possible to obtain a continuous record of the back- and forward-reflection regions. As in the improved Norelco spectrometer (see abstract by Hamacher and Parrish) the length of the focal spot is parallel to the specimen axis of rotation. Vertical Soller slits limit the divergence of the beam in the horizontal plane and the slit system is designed with adjustable divergence, scatter and receiving slits.

The angular aperture of 38′ for the range 10°–70° 2θ covers a 20 mm. wide sample at 10° 2θ. Since focussing is inherently better in the back reflection region, the angular aperture can then be increased to 4° at 70° 2θ to again cover the same width sample. In this way, intensities are increased and more precise measurements are possible. To achieve this larger angular aperture, the focal spot must be viewed at 3° in order to avoid using radiation between 0° (grazing incidence) and 1° to the target face because the intensity falls off rapidly in this region. The focal spot, 9×1.5 mm., is 9×0.07 mm. in projection at 3° so that the resolution is comparable with that achieved in the improved Norelco spectrometer. With the present design of x-ray tube, scanning angles up to 150° 2θ are reached and new tube designs indicate this may be considerably increased. Greater dispersion results from the larger radius (15 cm.) and the higher intensity source makes it possible to use an even larger radius if desired. The circuits are rack-mounted and the goniometer is designed to be attached to existing generator units.

DESIGN AND OPERATION OF GRID-CONTROLLED FINE-FOCUS *X*-RAY TUBE*

R. Pepinsky,
Alabama Polytechnic Institute.

A demountable fine-focus grid-controlled *x*-ray tube has been developed for stroboscopic diffraction studies of periodic lattice distortions. The control grid provides a simple means for turning on and off the tube current and hence controlling the *x*-ray emission, while the fine focal spot affords a great enhancement in the net intensity of a parallel-collimated beam of small cross-section.

The electron gun, comprised of a linearly-extended spiral filament, reflecting electrode, control grid, and focussing shield, is near ground potential to facilitate application of control voltages, and the target is at high positive potential. The grid cut-off voltage is about 35 volts, and its capacity with respect to the other electrodes is low to facilitate application of very short (0.1 microsecond) pulses. With the reflector about 100 volts negative and the focussing shield 200 to 300 volts negative with respect to the filament, a current of some 200 microamps at an accelerating voltage of 35 KV can be concentrated into a sharply-defined focal spot approximately 0.15 mm. high by 0.8 mm. long. Viewed at 3° from the target surface, the projected length reduces to about 0.04 mm. The specific target loading is about 75 watts/mm.^{2}

The fine focal spot permits the use of a single pinhole as a parallel-collimating device. An 0.005″ pinhole 12.5 cm. distant from the focus produces at the 3° grazing angle a beam of about 15′ divergence in the plane containing the long direction of the focal spot and the tube axis. This beam has the same intensity under DC excitation as that from a standard commercial diffraction tube, viewed at the same grazing angle, when the latter tube is operated at the same DC high voltage as the fine-focus tube but at 100 times the tube current.

The fine-focus tube thus provides a reduction by a factor of 100 in the input power required for a given average output intensity in a parallel-collimated beam of small cross-section. For periodically pulsed operation this results in extremely important reduction of the *peak* emission required from the cathode when the duty cycle (ratio of pulse length to repetition rate) is low and a beam of good *average* intensity is required.

Calculations are presented of permissible target loading under periodically pulsed excitation. These are based upon Bouwers'[1] calculations of loadings under short single pulse excitation, and upon the calculations and observations of de Graaf and Oosterkamp.[2] For low duty cycles at high repetition rates (50 to 100 KC) it is found that the *average* loading under pulsed operation can be as high as under DC excitation.

[1] Bouwers, A., *Zeit. techn. Phys.*, **8**, 271 (1927).

[2] de Graaf, J. E., and Oosterkamp, W., *Jour. Sci. Inst.*, **15**, 293 (1938).

THE ELECTRONIC FOURIER SYNTHESIZER*

R. Pepinsky,
Alabama Polytechnic Institute.

Three new developments are reported in the electronic Fourier synthesizer under construction at Auburn:[1]

[1] Pepinsky, R., *Jour. Appl. Phys.*, **18**, 601 (1947).

1. *Accurate* contour maps of electron densities or Patterson functions can be delineated directly on the presentation cathode-ray tube. This is accomplished by triggering coincidence circuits, set at predetermined voltage levels, directly from the synthesized voltage signal formerly applied for intensity modulation to the CR tube grid. The circuits produce 1-micro-second pips each time the synthesized signal crosses one of the preset levels, and these are applied to the CR tube grid in place of the entire synthesized signal.

As many of these contours as is desired can be delineated simultaneously on a map. These can be differentiated one from another by brightening or dotting various lines. The zero level of electron density can be set in through adjustment of the DC level of the synthesized signal.

The contouring technique was demonstrated on the model synthesizer previously shown at the CSA meeting at Annapolis, March 20, 1947.[2]

2. The restriction to centro-symmetric syntheses has been removed through the incorporation of sine as well as cosine terms. This was possible with addition of the required volume controls, switches and adding resistors, and by duplication of output portions of the 20 sine-wave oscillators only.

The possibility of non-centro-symmetric syntheses, combined with the obvious availability of one-dimensional syntheses, now afford rapid computation of general three-dimensional electron density and Patterson functions.

3. In combination with the synthesizer, a photoelectric procedure has been devised for computation of Fourier coefficients for two-dimensional functions, as defined by the relations:

$$\Omega_{H_1H_2} = \int_0^1 \int_0^1 \Omega \cos 2\pi(H_1s_1 + H_2s_2)ds_1ds_2 + i\int_0^1 \int_0^1 \Omega \sin 2\pi(H_1s_1 + H_2s_2)ds_1ds_2.$$

This depends upon preparation of photographic transparencies corresponding to Ω, and the multiplication and integration of these over a unit of Ω with a "fringe" corresponding to $\cos 2\pi(h_1s_1 + h_2s_2)$ or the corresponding sine. The fringes are available from the synthesizer, and the transparencies can be prepared by a radiographic technique.

The layout of the cosine and sine terms, on 42 panels ($19'' \times 36''$) of 40 terms each, and the general arrangement of the entire computer laboratory, are shown.

[2] Pepinsky, R., *Am. Mineral.*, **32**, 693 (1947).

OBSERVATIONS ON GEIGER COUNTER CHARACTERISTICS BY MEANS OF A GRID-CONTROLLED *X*-RAY TUBE[*]

R. Pepinsky and H. M. Long, Jr.,
Alabama Polytechnic Institute.

Control over the time of arrival of *x*-ray photons into a Geiger counter, as afforded by the grid-controlled *x*-ray tube reported in the preceding abstract, permits observations of importance in the theory and application of counter action.

1. Direct observation of dead and recovery times of counters, with simultaneous measurement of pulse heights and shapes in the recovery period. For example, under usual operating conditions the dead time in Norelco No. 62002 or 62003 counters is 100 microseconds; no photon arriving in a time less than this subsequent to a given counter discharge can be recorded as a pulse. Photons appearing later than 100 microseconds

after a count produce discharges which increase in height from zero at 100 microseconds to half maximum at 110 microseconds; and "full recovery," i.e., maximum pulse height, occurs at about 150 microseconds. A pulse height within the recovery period is related in a very definite way to the timing of the second photon.

2. Measurement of the time required for a photon-initiated discharge to reach the central wire, as a function of the distance of initial ionization from the wire. For the new Mica-window Norelco counters, e.g., and a beam parallel to the central wire and about 2 mm. distance from it, the counter pulse lags from 0.5 to 1.5 microseconds behind the arrival of the photon. This is presumably the time for collection of secondary electrons.

When the x-ray tube is periodically pulsed, the counter amplifying circuit can be gated off except during the times when discharges initiated only by x-ray pulses can appear. The background counts due to cosmic rays and radioactivity can then be very greatly reduced. In the present investigation a reduction by a factor of more than a hundred has been achieved.

Under self-quenching operation of the Norelco counters, scaling circuits with resolution times of less than 100 microseconds are unnecessary. For higher counting rates, resort is being had to counters of new design and to external quenching. Entirely reliable scalers with rates well in excess of a megacycle per second have been constructed, and it is recognized that properly-designed scaling circuits in themselves will not be the limiting factor in attainment of high resolution.

With the use of the entire fine focal spot as a source, as also described in the preceding abstract, it is possible to *meter* the photons issuing from one port of the x-ray tube by means of an auxiliary counter receiving a beam from an opposite port. The average deviation of the metered beam from a desired total number of photons can be reduced to any desired value by sampling a high enough number of counts in the monitoring beam. Direct measurements are presented of the statistics of this monitoring.

Circuitry for these observations is briefly described.

PREFERRED ORIENTATION AND SAMPLE PREPARATION FOR THE GEIGER-COUNTER SPECTROMETER

ANNETTE PRÉVOT AND GUENTER SCHWARZ,
The Johns Hopkins University.

We have been interested in the detection of small quantities of a light substance either pure or present in a mixture in low concentration.

The classical methods of sample preparation did not prove satisfactory for such a study. A holder, provided with a cavity to hold the sample, requires appreciable quantities of the substance. The use of a glass slide on which the sample mixed with a binder is spread causes a decrease in the absolute intensity of the diffracted beam due to the presence of the binder and an increase in the background due to scattering from the glass slide. The resultant increase in the statistical fluctuations makes it more difficult to distinguish weak lines from the background. In all standard methods, preferred orientation has to be prevented in order to obtain correct intensities of the diffracted lines.

Instead of avoiding preferred orientation we have been trying to produce it in order to favor one of the intense lines of the substance present in low concentration. The method we have used to create this preferred orientation has been to dissolve the substance under investigation and have the material recrystallize on the surface of the sample holder by evaporation of the solvent. The contribution to the background intensity due to the holder has been almost completely eliminated by supporting the sample on a very thin collodion film spread over a wire frame.

The method had been applied to dipentaerythritol (DiPE) either pure or mixed with pentaerythritol.

The study of mixtures led to the following results:

Ratio of $\dfrac{\text{most intense line of PE}}{\text{most intense line of DiPE}}$

% of DiPE	Cavity Holder	Crystallization
50%	2.0	0.3
5%	7.7	4

This technique has not given results sufficiently reproducible as to permit quantitative analysis of small amounts of DiPE, but must rather be considered as a method for the detection of impurities. Concentrations of DiPE as small as 1% can easily be detected. This corresponds to less than 0.1 mg of DiPE.

Some of the samples prepared from a 0.2% solution (absolute quantity of 20_γ DiPE) still show a DiPE line; whereas a relative amount of about 2% DiPE can be considered as the limit of sensitivity when a powder specimen is packed in a cavity holder.

A GRAPHICAL METHOD FOR TRANSFORMING RHOMBOHEDRAL MILLER INDICES AND HEXAGONAL BRAVAIS-MILLER INDICES

LEWIS S. RAMSDELL,
University of Michigan.

In some cases published data for rhombohedral crystals list only the rhombohedral Miller indices. In presenting new data there is sometimes an advantage in using both the Miller and the Bravais-Miller indices. Easy transformation from either set to the other is possible with the reciprocal lattice. Since the direct representation of a rhombohedral reciprocal lattice is difficult, it is common practice to treat the rhombohedral cell as a doubly centered hexagonal cell, with lattice points at 000; 1/3, 2/3, 2/3; and 2/3, 1/3, 1/3. The characteristic extinctions of this centered cell eliminate two-thirds of the corresponding reciprocal lattice points. Such a lattice, with only the points corresponding to the permissible rhombohedral reflections present, can be used both as a rhombohedral and a hexagonal reciprocal lattice. By the suitable choice of lattice directions, the indices *hkl* or *hkīl* can be determined directly for any point.

A COMPLETE STRUCTURE DETERMINATION

BARBARA ROGERS-LOW,
Harvard Medical School.

THE USE OF MICROWAVE DIFFRACTION IN STRUCTURE ANALYSIS

WALTER L. ROTH,
General Electric Company.

Preliminary tests of the possibility of utilizing microwave diffraction from molecular models as an adjunct to crystal structure analysis have led to the following conclusions.

Commercial oscillators of 3750 Mc. and 24000 Mc. frequency (8 and 1.2 cm. wave length) generate sufficient power for studying diffraction phenomena. The use of superheterodyne reception provides sensitivity sufficient to detect the radiation scattered from

a small object, such as might be used to represent a single atom. Background radiation can be reduced with quarter-wavelength absorbers to an extent adequate for experimental work within the confines of an ordinary laboratory room. Diffraction patterns easily are observed by rotating a parabolic receiver about the diffracting cell, and measuring the intensity received as a function of angle. The intensity distribution in a cross section taken through a beam generated from a paraboloid or lens is not sufficiently constant to permit the vector addition of amplitudes from points within the unit cell by conventional methods, which require a wave front constant in both phase and intensity across the cell.

A new type of radar antenna has been designed, the basic feature being the incorporation of both phase and intensity control of the source. To be of practical use for the solution of molecular structure problems, the beam should be constant in amplitude to several per cent over an area of at least one square foot (corresponding to a unit cell). Calculations indicate that a beam with the required characteristics can be produced, but precision apparatus probably requiring several years development is necessary. Since the projected applications to molecular structure problems do not appear to warrant such extensive development, the project has been discontinued.

The experimental work was carried out largely by Miss Gabrielle Hamburger, with the assistance of Mr. Richard Koch who developed and assembled the necessary electronic circuits.

THE CRYSTAL STRUCTURE OF A METANILAMIDO-PYRIMIDINE

JOSEPH SINGER* AND I. FANKUCHEN,
Polytechnic Institute of Brooklyn.

The structure of 2-metanilamido-5-Br-pyrimidine has been worked out by two-dimensional Patterson and Fourier methods. The isomorphism of this compound with its iodine analogue was of assistance. The chlorine analogue has a different crystal structure. The lattice constants, as indexed for $P2_1/n$, are:

	a	b	c	β
Bromine:	9.53	5.64	21.9	92.5°
Iodine:	9.70	5.67	22.0	92.5°

About 75% of the $0kl$ structure factor signs were determined by successive trials in the usual way. The ring details remained unclear, however, until a subtraction-Fourier device was hit upon. A Fourier series using coefficients given by $(F_{0kl}^{obs} - F_{0kl}^{Br})$, where the temperature corrected Br contribution is subtracted from the observed F_{0kl}, gave sufficient detail to allow most of the remaining signs to be determined. Two trials resulted in a fairly clear Fourier projection and the intensity checks are good. The subtraction apparently works because the high order terms are emphasized. Absolute intensities are required. A second projection, $h0l$, is being worked on. At this point, several bond angles and bond lengths are already determined and lie within expected figures.

* At present with Franklin Institute, Philadelphia, Pa.

ANALYSIS OF TWINNED INTERGROWTHS OF CRYSTALS

C. B. SLAWSON,
University of Michigan.

All the crystal planes of two or more twinned individuals may be referred to the crystallographic axes of one of them. Every plane will have rational indices on the common axes. Equations are developed for transforming the indices. The forms resulting from some common twinning laws are presented in tabular form.

The juncture surfaces between twins may be (1) the twinning plane, which is crystallographically continuous, with no free energy at the interface, or (2) an interface of planes with unlike indices and free energy at the interface. The second type of juncture occurs in contact twins at the points of discontinuity if the twinning plane is step-like, and in all penetration twins. These suture junctions are surfaces of weakness and also commonly the locus of flaws and inclusions.

The potential twinning plane may be (1) a single layer of atoms which may be considered as common to both individuals, or (2) a double layer of atoms both of which may be common to each individual. An example of the single layer type would be a simple cubic structure twinned across the octahedron with the bonds inclined to the twinning plane while the tetrahedral-bonded diamond or sphalerite would be of the double layer type with the bonds between the layers normal to the twinning plane. One would therefore not expect to see twinning in the first type and would expect it to be common in the second type, as is the case with diamond, sphalerite, and fluorite. This results from the energy distribution on the twinning plane of the double layer type.

ELECTRON DIFFRACTION STUDIES OF MANGANESE PRECIPITATION IN MAGNESIUM ALLOYS

LORENZO STURKEY,
Dow Chemical Company.

Manganese occurs either as an impurity or as a deliberately added constituent in practically all commercial magnesium alloys. Concentrations range from a few hundredths of a per cent in cell magnesium to something over one per cent in alloys containing no aluminum. It has been shown that many of the properties—especially grain size and corrosion characteristics—are directly connected with the composition and amount of manganese precipitation. Electron diffraction studies have been made using selective etching techniques[1] to study this precipitation, with the following results:

(a) *Magnesium plus 1–2% Mn (either with or without Ce)* contains α-Mn precipitation.

(b) Mg 1 Zn, 0–0.4 Fe, 0–0.3 Al, 0–0.4 Mn (rolled sheet): Mn is precipitated in one of the various Mn-Al compounds, depending upon the Mn to Al ratio in the alloy. β-Mn occurs at the composition containing 0.3% Al and 0.40% Mn with a 2% increase in the lattice constant of β-Mn.

(c) Cell magnesium, which contains other metallic elements as impurities only, shows Mn precipitation either as a Mn-Al phase or a Mn-Al-Cu phase when Al and Cu are present, even in quantities less than 0.01%.

(d) *Commercial Mg-Al-Zn alloys containing from 0.1–0.3% Mn:* Mn is present in the cast metal as $MnAl_6$ crystals unless the melt has been superheated. Single crystal patterns of a "cross-grating" nature from these $MnAl_6$ crystals are frequently obtained and may be used for structural and crystal habit information.

Superheated melts showing grain refinement when cast contain a different Mn precipitation of such a nature as to increase nucleation of magnesium crystals. Rolling or heat-treatment after casting usually results in additional $MnAl_6$ precipitation.

[1] Heidenreich, Sturkey, and Woods, *Jour. Appl. Physics*, **17**, 127 (1946).

FORMATION OF KCl CRYSTALS FROM AN AQUEOUS SOLUTION AT VARYING RATES OF EVAPORATION

HELMUT THIELSCH,
Lehigh University.

Crystallization of a substance can be described in terms of nucleation and crystal growth. However, depending upon the rates of the two phenomena, principally the latter,

distinctly different crystal patterns (crystal habit) may be produced. These have been studied in aqueous solutions in which the rates of nucleation and crystal growth were varied by changing the rates of evaporation of the water phase. This was accomplished with the aid of an efficient vacuum system.

Thus tests made on KCl aqueous solutions showed[1] that slow rates of crystallization will produce relatively few crystals having well developed cubic faces. This, of course, is in agreement with the theories of Stranski, Kossel and Volmer[2] who predict such formation under (or near) equilibrium conditions. The ions will deposit in tangential fashion building up orderly plane upon plane.

Above a definite rate of evaporation the KCl ions deposit in a linear dendritic pattern. This is due to temperature gradients from the released heat of fusion (or crystallization) which prevents crystal growth on the faces of the crystallites. Still faster rates of evaporation will produce a region in which crystallization occurs in an irregular dendritic pattern. Here ionic movement or migration may be restricted by extreme concentration currents. However, the resulting structure is still cubic in nature.

With maximum rates of evaporation the ions are not able to fall into a regular lattice arrangement. Instead, they "freeze" virtually in the positions which they held last in the liquid solution. This is the familiar amorphous state.

Only the first arrangement is thermodynamically stable. In the other three ion migration or reorientation will occur when the specimen is heated or is allowed to remain in a moist atmosphere for several days. These conditions will supply sufficient energy to the KCl ions allowing their rearrangement into the stable cubic lattice pattern.

Impurities present in the aqueous solution which are either insoluble, or due to their quantity or lower solubility will form nuclei ahead of the principal (KCl) substance, will act as seed crystals. The presence of these will increase the rate of crystallization tending to support growth in dendritic patterns instead of the equilibrium cubic planar structure. Moreover, the "foreign" atoms or ions will interfere with the migration phenomena, making it less likely for these dendrites to rearrange. This, however, depends on the amount and kind of impurities present and the "reorientation" energy supplied.

[1] Thielsch, H., *Jour. Chem. Phys.*, **13**, 249 (1945).

[2] Volmer, M., "Kinetic der Phasenbildung," Verlag von Theodor Steinkopff, Dresden und Leipzig (**1939**).

PUNCHED CARD METHODS OF FOURIER ANALYSIS

L. H. THOMAS,
Watson Scientific Computing Laboratory.

The summation of numerical Fourier series may be done by standard punched card methods, at a speed depending on the rate of the slowest operation, multiplication. There are three methods of carrying out the multiplications required.

I. Using tables on cards of multiples of sines and cosines requires the minimum of equipment. A key-punch, sorter, and tabulator suffice; though a considerably smaller file of cards is required if a reproducer and summary punch is available. The equivalent of about 3000 multiplications per hour to six digit accuracy can be attained.

II. Multiplying by progressive digiting requires only tables on cards of sines and cosines; and key-punch, sorter, tabulator, and reproducer and summary punch. About the same speed of 3000 six digit multiplications an hour is possible for sums of 30 or more products.

III. Multiplying by machine is more flexible but requires a multiplying punch. With the new "603" multiplier, 6000 six digit multiplications can be done per hour. For all these methods a collator is useful but not essential.

There are available at the Watson Laboratory tables on cards for doing crystal structure Fourier analysis by method I. These consist of tables of A cos $(mn(2\pi/3))$ and A sin $(mn2\pi/3)$, $n=0$, 1, 2, 3 on the same card; for $m=0$, 1, 2, 3 and $A=-499000$ to 500000 by 1000 and from 1 to 999 by 1, values given to seven figures; 12000 cards: and corresponding cards for A cos $(mn2\pi/5)$ and A sin $(mn2\pi/5)$; 20000 cards. A complete three dimensional $60\times60\times30$ Patterson to five digit over-all accuracy can be done with these cards by the method of sub-series in five to seven weeks.

Tables on cards are being computed and will soon be available of cos z and sin z to six decimals and of sin z/z to five decimals with $z=2\pi rs/400$, $s=1$, 2, $\cdots$ 600; $r=1$, 2 $\cdots$ 200, for doing Fourier analysis by method II or method III.

OBSERVATIONS ON PIEZOELECTRIC CRYSTALS

Karl S. Van Dyke,
Wesleyan University.

Considerable thought has been given to tabulating the piezoelectric, dielectric and elastic properties of crystals for piezoelectric application. A scheme for systematic portrayal of the constants of the several properties by crystal classes, and for presenting the numerical values of the constants for ready use in piezoelectric equations of the bilinear type, has been developed. Calculations of the tables, or matrices, of constants has been carried out as part of a research program supported by a Signal Corps contract and has been completed for several commonly used crystals. The constants are given for all four of the forms of the basic equations (solved for any two of the four variables: stress, strain, field and electric displacement), taking the basic data from the literature. The data completed so far are incorporated in Part II of a report of January 20, 1948 to the Signal Corps as a volume entitled *A Manual of Piezoelectric Data* under the author's name. Data on additional crystals will be given in a second volume in July 1948.

Two other parts of this Signal Corps supported research may be of special interest to crystallographers. These are both treated in a Master's Degree thesis by Clyde P. Glover, appear in earlier reports to the Signal Corps and have been presented to the American Physical Society. One of these is the peculiar characteristic etching of a Z-cut plate of quartz by hydrofluoric acid when a field of five to ten thousand volts per millimeter is applied across the etching surface, following a technique used by Choong in China. Growth rings appear on the surface of the quartz, usually as nearly concentric triangles showing a preference for growth on major rhombs. The etching alternates within and between the triangular annuli among two characteristic types. These same two types of quartz are distinguishable in the selective blackening of quartz under x-ray illumination. The boundaries between regions under the two types of development coincide. Again, measurement of the optical density of x-irradiated quartz and of the coincident elastic defect, both as functions of the radiation time, shows the two phenomena to be different functions of the radiation, and the elastic defect to saturate at about half the irradiation which saturates the blackening.

PHOTOELASTIC PROPERTIES OF CRYSTALS

C. D. West and A. S. Makas,
Polaroid Corporation.

Elastic behavior of a solid can be visualized by specifying the dimensions of the triaxial strain ellipsoids which result from the deformations of an initial unit spherical element by applications of unit stresses; these dimensions are given through the elastic compliances s_{ik}. Similarly, photoelastic behavior of a transparent solid is visualized by specifying the

changes in the triaxial index ellipsoid which result from applications of unit stresses; these are given through the photoelastic compliances $\bar{\pi}_{ik}$. From these two sets of material constants are derived the dimensionless photoelastic strain constants $\bar{p}_{ik}$ which show the optical effects accompanying unit strains. Data taken from the literature illustrate the very wide range of these three sets of constants for type materials (see Table 1, which includes for comparison the flow birefringence constant of a liquid containing highly anisotropic molecules). In general one gets the maximum birefringence per unit stress from the weakest solids, but the maximum per unit strain from the strongest solids.

TABLE 1. ELASTIC AND PHOTOELASTIC CONSTANTS UNDER SHEAR STRESS

Material	Elastic Compliance $1/G = 2(s_{11} - s_{12})$ in 10^{-13} cm^2/dyne	Photoelastic Compliance $2B/n^3 = (\bar{\pi}_{11} - \bar{\pi}_{12})$ in 10^{-13}cm^2/dyne	Photoelastic Strain Constant $\frac{1}{2}(\bar{p}_{11} - \bar{p}_{12})$
Diamond	3.58	0.78	0.225
MgO	9.82	1.24	0.126
CaF$_2$	16.8	1.42	0.086
LiF	27.0	1.44	0.053
Silica Glass	32.4	1.91	0.059
K alum	137	5.0 (av.)	0.037 (av.)
Bakelite, 21° C.	645	20.8	0.0323
Bakelite, 110° C.	358,000	558	0.00156
13% Aq. Gelatine Gel	72,500,000	44,600	0.000615
Range	(10^7)	(10^4)	(10^3)
Nitrobenzene in laminar flow, 20° C., $\eta = 0.02$ poise		2,300	—

A more extensive survey of photoelastic behavior of solids would soon remove any illusion of regularity and reveal it be a highly capricious phenomenon—the $\bar{\pi}$ constant corresponding to a known s constant can be large or small in magnitude, positive or negative in sign, without any immediately obvious reason.

Isotropic bodies and trigonal and hexagonal crystals have one easily measured constant of stress birefringence ($\bar{\pi}_{11} - \bar{\pi}_{12}$); cubic and tetragonal crystals have two such constants ($\bar{\pi}_{11} - \bar{\pi}_{12}$) and $\bar{\pi}_{44}$ resp. $\bar{\pi}_{6s}$, and the greater the difference between these two constants, the higher is the photoelastic anistropy of the crystal. We have measured approximate constants for cubic crystals which illustrate high photoelastic activity and anistropy as follows:

TABLE 2. PHOTOELASTIC ANISTROPY OF CUBIC CRYSTALS

Crystal	λ (mmu)	n	$\bar{\pi}_{11} - \bar{\pi}_{12}$	$\bar{\pi}_{44}$
AgCl	560	2.08	−5.62	+8.89
Tl(Cl, Br), or KRS-6	560	2.36	(0)	−13.1
Tl(Br, I), or KRS-5	610	2.62	(−4)	−27.2

A known photoelastic anistropy can be utilized in locating crystallographic directions in a crystal block, in interpreting pressure figures observed polariscopically, and the like. An annealed plate of polycrystalline AgCl in tension reveals some grains with positive,

others with negative birefringence—this is understandable only in view of the opposite signs of its two constants as tabulated. The same plate in transverse torsion or bending also reveals birefringence which now is confined to the vicinity of such grain boundaries as are not perpendicular to the plane of the plate—this likewise new phenomenon can also only be understood in terms of photoelastic anistropy. Such photoelastic effects observed in poly-crystalline plates of the cubic system one should be able to duplicate without difficulty in cemented models formed from unlike plastics (isotropic bodies) and study more conveniently in this way. A knowledge of photoelastic constants would seem to be necessary for interpreting the complex permanent birefringences observed in cubic crystals to result from plastic deformations.

CRYSTALLIZATION OF POTASSIUM NITRATE

V. C. Williams, L. O. Stine, and R. M. Garrels,
Northwestern University.

Potassium nitrate was crystallized from aqueous solutions in a small vacuum crystallizer under constant pressure and constant stirring conditions. Temperature-time curves for the crystallization were obtained, and data on crystal size procured by photographic sampling at regular time intervals. A plot of average crystal size against time gave a linear relationship; extrapolation to the time of zero size was made for comparison with the cooling curves. The time at which crystallization began, as indicated by this extrapolation, occurs several minutes before any heat effects, indicating that the linear growth does not occur until equilibrium is reached, and that growth prior to equilibrium is very rapid. Equilibrium was reached at an average size of approximately 0.1 millimeter; after this size was attained little further free nucleation occurred. The rate of cooling of the supersaturated solution was 1.5 times the rate after equilibrium was attained; rough calculations from the data available in the literature indicate a heat of crystallization of approximately 30–35 calories per gram. This is roughly one-half the heat absorbed during solution under nearly corresponding conditions; that is, from crystals to saturated solutions. The number of nuclei present at equilibrium in these experiments was about one per cubic millimeter, or 100,000 per 100 cubic centimeters of solution. The experiment was originally designed to secure data on the change of heat of crystallization with size, on the hypothesis that the very small sizes, because of increased surface energy, should show smaller heat effects. The variation was not detected, but difficulty in securing formation of enough nuclei may have obscured the effect.

INFORMATION CONCERNING THE WATER UPTAKE OF COLLAGEN AS EVIDENCED BY ITS LOW ANGLE *X*-RAY DIFFRACTION PATTERN

Barbara A. Wright,
Research Division, United Shoe Machinery Corp.

A series of low angle *x*-ray diffraction patterns of collagen were photographed under controlled conditions of humidity, temperature, and tension. A specially designed specimen holder was attached to our North American Philips low angle *x*-ray diffraction camera. Relative humidities from 2% to 100%, and temperatures from 20° C. to 100° C. can be maintained in this holder and various controllable amounts of tension can be applied to the sample. All patterns in this series were taken on the same sample of kangaroo tail tendon stained with phosphotungstic acid. These patterns show variations both in the fundamental collagen spacing and in the relative intensities of the observed orders as a function of relative humidity. No changes in the pattern were produced by variations in temperature from 20° C. to 70° C. A marked reduction of the over-all intensity of the diffraction

pattern occurs above this temperature range only at high humidities. Possible alterations in the collagen molecular structure which could account for these observations will be discussed.

SOME CRYSTALLINE HEMOGLOBINS

DOROTHY WRINCH,
Smith College.

The classical study of crystalline hemoglobins by Reichert and Brown provides several instances of cubic and hexagonal crystals, many instances of such "pseudo-symmetries." Since x-ray studies afford many examples in which such "pseudo-symmetries" indicate a direct approach to the atomic pattern,[2] these instances may well provide pointers to the structural principle in which the protein essence resides. A preliminary analysis of two such instances follows:

I. Oxyhemoglobin of Albino of Mus norvegicus (p. 230).[1]

Orthorhombic. Axial ratio: $a:b:c = 0.7829:1:0.7332$. Since $a:b:c = 1/\sqrt{2} \times 1.05:0.95$ $:1/\sqrt{2} \times 0.985$, a companion cell may be taken with unit displacements $[110]_c$, $[002]_c$, $[1\bar{1}0]_c$ in the cubic system $x_c y_c z_c$ from which the actual cell differs in its cell ratios by not more than ± 5 per cent. Since $2x = x_c + y_c$, $2y = z_c$, $2z = x_c - y_c$, we may rewrite these relations and interpret the recorded forms as follows:

$$(200) = (110)_c, \qquad (020) = (001)_c, (002) = (1\bar{1}0)_c;$$
$$\text{unit prism } (110); \quad (220) = (111)_c, (2\bar{2}0) = (11\bar{1})_c;$$
$$\text{brachydome } (011); (022) = (1\bar{1}1)_c, (0\bar{2}2) = (1\bar{1}\bar{1})_c.$$

Thus the companion cell has the single cubic form $w(111)_c$. Trillings in parallel on the unit prism as composition face are recorded. These the companion cell identifies as $(w/3)$ trillings.

II. Oxyhemoglobin of Ursus americanus (p. 259).[1]

Monoclinic. Axial ratio: $a:b:c = 1.2239:1:1.1429$, $\beta = 75°5'$. The forms recorded are $(\bar{1}11)$, $(1\bar{1}0)$, (010), (001) and in twins $(2\bar{3}0)$. Since $a:b:c = \sqrt{6}/2 \times 1.03:1.03:\sqrt{6}/2 \times 0.97$, a companion cell may be taken with unit displacements $[11\bar{1}]_c$, $[\bar{1}10]_c$, $[111]_c$ in the cubic system from which the actual cell differs in its cell ratios by not more than ± 3 per cent and in angle by $4°33'$, affording the following interpretations:

$$(400) = (11\bar{2})_c, (020) = (\bar{1}10)_c, (004) = (112)_c:$$
$$(\bar{2}22) = (\bar{1}12)_c, (22\bar{2}) = (\bar{1}1\bar{2})_c, (1\bar{1}1) = (100)_c, (\bar{1}\bar{1}\bar{1}) = (0\bar{1}0)_c:$$
$$(2\bar{3}0) = (1\bar{2}1)_c, (2\bar{3}0) = (2\bar{1}\bar{1})_c: (440) = (\bar{1}3\bar{2})_c, (\bar{4}40) = (\bar{3}12)_c.$$

The measured angles correspondingly pass into angles of the cubic system.

(1) $78°30' = \bar{1}\bar{1}0{-}001 \wedge 1\bar{1}0{-}001 = (1\bar{3}2)_c{-}(112)_c \wedge (3\bar{1}\bar{2})_c{-}(112)_c = \cos^{-1}(1/5) = 78°28'$:

(2) $79° = 1\bar{1}0 \wedge 001 = (3\bar{1}\bar{2})_c \wedge (112)_c = \cos^{-1}(1/\sqrt{21}) = 77°24'$:

(3) $46°47' = \bar{1}11 \wedge 00\bar{1} = (\bar{1}12)_c \wedge (\bar{1}\bar{1}\bar{2})_c = \cos^{-1}(2/3) = 48°11'$.

Twins, in trillings with c as common axis and composition face $(2\bar{3}0)$ are recorded. These are translated into $(w/3)$ trillings with common axis $[111]_c$ and composition faces $(2\bar{1}\bar{1})_c$, $(\bar{1}2\bar{1})_c$, $(\bar{1}\bar{1}2)_c$.

These two cases, and many others which can be analyzed in similar fashion, suggest the following conclusions. The hemoglobin crystals contain a dominant cubic theme,[2] to which

---

[1] The Crystallography of Hemoglobins. Carnegie Institution of Washington (**1909**).

[2] Wrinch, Dorothy, *Am. Mineral.*, **32**, 695 (1947).

the close approach of the crystal lattices to compound cubic lattices is due. This theme is associated with the submultiple cube, thus being closely definable in scale and in orientation. However the cubic theme is disturbed, in definite ways, by a minor non-cubic theme (since the crystal lattices are in fact not compound cubic lattices) though not so far as to be unrecognizable. It must be presumed, if these conclusions prove correct, that the dominant major theme comprises cubic skeltons of protein molecules and that the minor theme is the distribution of substituents or side chains on the molecular skeltons.
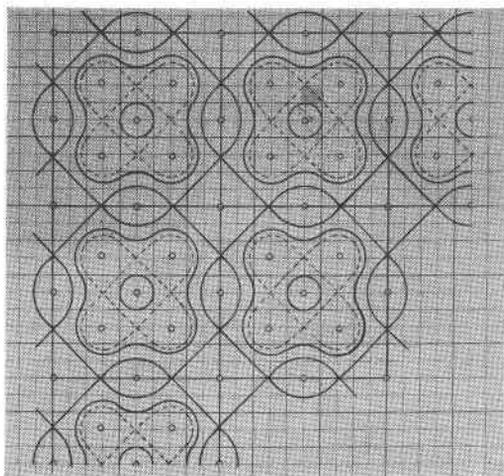

Fig. 1

AN APPLICATION OF FOURIER TRANSFORMS TO A CRYSTAL STRUCTURE ANALYSIS

Dorothy Wrinch,
Smith College.

In an ASXRED Monograph,[1] a discussion of Fourier transforms has been given, with a view to their wider use in x-ray structure analysis. This note traces an application of these ideas to a crystal for which a complete structure analysis has been given,[2] namely pentaerithrytol $C(CH_2OH)_4$ which crystallizes with space group $I\bar{4}$ and $a = 6.10$ Å, $c = 8.73$ Å. While the procedures can be applied to the three-dimensional molecule, only the F_{hk0}'s will be considered. The extension to three dimensions introduces no new principle.

We adopt a crude representation for the molecule and take 9 points for its tetragonal projection, viz. $x_i y_i = 00$, $\pm(10)$, $\pm(01)$, $\pm(20)$, $\pm(02)$ on a square lattice of metric k, thus adopting, for the C-C and C-O bonds indifferently, a length $a = k\sqrt{6}/2$. Then:

$$T(XY) = 1 + 2\cos^2 \pi X + 2\cos 4\pi X + 2\cos^2 \pi Y + 2\cos 4\pi Y$$
$$= 4(\cos 2\pi X + 1/4)^2 + 2(\cos 2\pi Y + 1/4)^2 - 7/2.$$

Thus T has a square lattice with unit displacements $XY = 10,01$ (cp. Fig. 1). The map has just one important "parameter" $X_1 = \cos^{-1}(-1/4) = 0.290$. On the diagonals of

[1] Wrinch, Dorothy, Fourier Transforms and Structure Factors (**1946**).
[2] Llewellyn, F. J., Cox, E. G., and Goodwin, T. H., *J. Chem. Soc.*, 883 (**1937**).

the square, it marks the minimum $T = -7/2$, on the edges the col $T = 11/4$, on the line $Y = 1/2$ the col $T = -5/4$. The general topology of the transform is then determined. To draw contours to any degree of fineness it is necessary and sufficient to compute $\cos^2 \pi X$ $+\cos 4\pi X$ correspondingly: the points in which the contours hit the diagonals; edges and the lines $Y = 1/2$ are then known.

With the transform drawn to any convenient scale, the scale in reciprocal space is fixed. If the unit cell has edge (say) 10 cm., then on our map 10 cm. means $d^* = 1/k$. With $a = 1.5°$ Å, for example, 10 cm. would mean $d^* = 1/1.225$ Å. With suitable values of k in mind (e.g. 1.225 Å), we compare the map with the map of F_{hk0} on the same scale, placing the origin on any node of the transform. Rotating one relative to the other changes the mutual orientation of the molecule and the crystal. Our objective, of course, is to find—with some small latitude in k—the orientation which will place large F's in regions in which $|T|$ is large, whether positive or negative and small F's in regions where $|T|$ is small. This we find is achieved in large measure by orienting the intensity map at $\tan^{-1}(4/3)$ to the axes of the molecules, with the identification $XY = 20$, $hk = 86$. We therefore write: $h = 4X - 3Y$, $k = 3X$ $+4Y$; $25x = 4x_t - 3y_t$, $25y = 3x_t + 4y_t$; thus obtaining for the atomic positions

carbon $(x_t y_t = 10)$ $xy = 0.16, 0.12$: oxygen $(x_t y_t = 20)$ $xy = 0.32, 0.24$.

These may be compared with the atomic positions derived from the Patterson map and with those finally adopted after the complete structure analysis,[2] viz.

$$\text{carbon } xy = 0.161, 0.123; \text{ oxygen } xy = 0.314, 0.247:$$
$$xy = 0.162, 0.123; \qquad\qquad xy = 0.317, 0.247.$$

It should also be recorded that, when we assign to each F the sign of the region of the transform in which it finds itself, 46 of the 48 signs are those adopted in the structure analysis.[2] The two F's in question are $F_{400} = 5.3$ and $F_{730} < 2.8$ and $F_{060} = 148$. We could then, of course, proceed in the usual manner, no longer focussing attention on the atomic positions yielded by the extremely crude representation of the molecule through the transform and so obtain a Fourier synthesis in atomic space practically indistinguishable from the distribution found in the structure analysis.

In this example of the actual use of Fourier transforms, the following points may be emphasized. (A) The representation used for the molecule is extremely crude in that (1) atomic scattering factors are neglected, i.e. atoms are represented by points, (2) carbons and oxygens are not distinguished, i.e. each point has the same weight, (3) C-C and C-O bonds are given a common length. (B) The resulting transform is then extremely simple and can be computed within the hour. (C) Despite the crudeness of the transform the xy parameters for the atoms are found within 3 per cent and the signs adopted for the F's are correctly assigned in almost all cases. It may therefore be claimed that, regarded as a preliminary to the stage of the refinement of parameters, the use of a Fourier transform can be both efficient and swift.

CRYSTAL CHEMISTRY OF THE ELEMENTS
FROM ACTINIUM TO AMERICIUM

W. H. ZACHARIASEN,

Argonne National Laboratory and Department of Physics,
University of Chicago.

During and after the war crystal structure studies have been carried out on a number of compounds of actinium, thorium, uranium, neptunium, plutonium and americium.

Most of the investigated compounds correspond to the tetravalent or trivalent states. The

structures deduced for these compounds indicate that the binding is predominantly ionic in character. Table 1 shows the ionic radii of the trivalent and tetravalent ions for co-ordination number six. The radii were deduced from observed distances in oxygen and fluorine compounds using ionic radii of 1.40 Å for O^{-2} and 1.33 Å for F^{-}. The monotonic decrease of ionic radius with increasing atomic number represents experimental proof that the added electrons enter the $5f$-shell.

A similar decrease in the size of the $(XO_2)^{+2}$-radical is observed in passing from uranyl to neptunyl to plutonyl compounds.

In the subnormal valence states the variation of crystal radius with increasing atomic number shows irregularities which are not understood at present.

TABLE 1. IONIC RADII

Number of $5f$-Electrons	Thoride Series	Actinide Series
0	Th^{+4} 0.95 Å	Ac^{+3} 1.11 Å
1	Pa^{+4} (0.91)	$(Th^{+3}$ 1.08)
2	U^{+4} 0.89	$(Pa^{+3}$ 1.06)
3	Np^{+4} 0.88	U^{+3} 1.04
4	Pu^{+4} 0.86	Np^{+3} 1.02
5	Am^{+4} 0.85	Pu^{+3} 1.01
6		Am^{+3} 1.00

CRYSTAL CHEMICAL RELATIONS IN INORGANIC PIEZOELECTRIC MATERIALS

SAMUEL ZERFOSS,
Naval Research Laboratory.

Increased interest in specialized electronic gear has resulted in a renewed search for new synthetic piezoelectric materials. The war-time production of large single crystals of $NH_4H_2PO_4$ is a notable example. The Crystal Section of the Naval Research Laboratory has undertaken a comprehensive laboratory survey of piezoelectric materials and has completed the testing of all the likely water soluble inorganic compounds which were obtainable in the necessary form. The purpose of this paper is not to present the detailed experimental data of that investigation but to summarize some of the general relations observed. Wooster[1] has listed the simple crystal chemical relationships found to exist in piezoelectric inorganic salts. He showed for example that the majority of the piezoelectric materials contain a radical which does not possess a center of symmetry. The more complete data of the present investigation are used in an attempt to extend these relationships and to account for the various exceptions.

[1] Wooster, Crystal Physics, Cambridge (**1938**).